Draft Risk Evaluation for Octamethylcyclotetrasiloxane (D4)

Supplemental Information File:

Evaluation of Campbell 2023 PBPK Model for Octamethylcyclotetrasiloxane (D4)

CASRN 556-67-2

28	MEMOI	RANDUM CONTRACTOR OF THE PROPERTY OF THE PROPE
29		
30	Date: 9/2	26/2024
31		
32	SUBJEC	CT: Evaluation of Campbell 2023 PBPK Model for Octamethylcyclotetrasiloxane (D4, CASRN
33		556-67-2)
34		
35	FROM:	ICF
36		
37	TO:	United States Environmental Protection Agency

TABLE OF CONTENTS

SUMMARY	••••••
1 BACKGROUND INFORMATION	••••••
1.1 Physicochemical Properties	
1.2 Absorption, Distribution, Metabolism, and Excretion (ADME) and Pharmac	odynamic
Considerations	
1.3 Toxicity of D4	
1.3.1 Summary of D4 Toxicity in Humans	
1.3.2 Summary of D4 Toxicity in Animals	
1.4 Regulatory History of D4	
1.5 D4 PBPK Models	
1.6 Model Data	
2 MODEL PURPOSE	
3 MATERIALS AND METHODS	
3.1 Modeling Strategy	
3.2 Summary of Data for Model Development and Evaluation	
3.3 Model Development and Structure	
3.4 Model Equations	
3.4.1 Arterial Blood	
3.4.2 Venous Blood	
3.4.3 Lung	
3.4.5 Liver	
3.4.5 Livel 3.4.6 Rapidly Perfused Tissues	
3.4.7 Slowly Perfused Tissues	
3.4.8 Oral Dosing	
3.4.9 Dermal Exposure	
3.5 Model Parameters	
3.6 Model Simulations	
3.7 Software	
4 MODEL RESULTS	3
4.1 Model Evaluation	3
4.2 Sensitivity, Uncertainty, and Variability Analyses	
4.3 Model Applicability	
5 DISCUSSION AND CONCLUSIONS	
6 LIST OF ELECTRONIC FILES AND SUPPORTING DOCUMENTS	
REFERENCES	
KEFEKENCES	5
LIST OF TABLES	
Table 3-1. List of Prefixes Used in the Model	
Table 3-2. List of Abbreviations Used in the Model	
Table 3-3. Physiological Parameters for the D4 PBPK Model	

80	Table 3-4. List of State Variables, Non-Constant, and Other Model Parameters
81	Table 4-1. Sum of Squared Errors for the Campbell 2017 and 2023 Models Compared with Inhalation
82	Data in F344 Rats
83	Table 4-2. D4 PBPK Model Input Parameters That Result in a Normalized Sensitivity Coefficient of 0.2
84	or Greater in Listed Compartments (Blood, Liver, Fat, and Lung) of F344 Rat at the End of 28-
85	day Inhalation Exposure and the End of 14-day Postexposure Period
86	Table 4-3. D4 PBPK Model Input Parameters That Result in Normalized Sensitivity Coefficient of 0.2
87	or Greater in Listed Compartments (Blood, Liver, Fat, and Lung) of SD Rat at the End of 28-
88	day Exposure and the End of 14-day Postexposure Period
89	Table 4-4. D4 PBPK Model Input Parameters That Result in a Normalized Sensitivity Coefficient of 0.2
90	or Greater Listed Compartments (Exhaled Breath, Plasma) of Human Male at the End of
91	Dermal Exposure and the End of Postexposure Period
92	Table 4-5. D4 PBPK Model Input Parameters That Result in a Normalized Sensitivity Coefficient of 0.2
93	or Greater in Listed Compartments (Exhaled Breath, Plasma) of Human Male at the End of
94	Inhalation Exposure and the End of Postexposure Period
95	Table 4-6. D4 PBPK Model Input Parameters That Result in a Normalized Sensitivity Coefficient of 0.2
96	or Greater in Listed Compartments (Exhaled Breath, Plasma) of Human Male at the End of
97	Oral Exposure and the End of Postexposure Period
98	
99	LIST OF FIGURES
100	Figure 3-1. Conversion of MLP from (a) Unidirectional to (b) Bidirectional Compartment
101	Figure 3-2. PBPK Model Diagram for Rat and Human Adapted from {Campbell, 2023,
102	11778986@@author-year}
103	Figure 4-1. Comparison of Model Simulations and F344 Rat Inhalation Experimental Data
104	Figure 4-2. Comparison of Model Simulations and Male F344 Rat Oral Experimental Data
105	Figure 4-3. Comparison of Model Simulations and Human Inhalation and Dermal Data
106	Figure 4-4. Comparison of Model Simulations with Human Dermal Data from Two Datasets
107	Figure 4-5. D4 Concentrations in Plasma from Human Oral Experimental Data
108	Figure 4-6. Simulation of Repeated-Dose Oral Exposure in Humans
109	Figure 4-7. Venn Diagram Illustrating the Distribution of Sensitive Parameters by Exposure Route 51

SUMMARY

- 111 The U.S. Environmental Protection Agency (EPA) initiated review of a physiologically-based
- pharmacokinetic (PBPK) model for use in assessment of risk to humans exposed to
- octamethylcyclotetrasiloxane (D4). The regulatory purpose of the D4 PBPK model is for use in the risk
- evaluation of D4, conducted pursuant to the Toxic Substances Control Act (TSCA) as amended by the
- Frank R. Lautenberg Chemical Safety for the 21st Century Act. Under this law, EPA evaluates potential
- risks from existing chemicals and acts to address any unreasonable risks chemicals may have on human
- health and the environment.

118

110

- D4 is a low molecular weight methyl siloxane that is used in the production of silicone polymers.
- 120 Silicone polymers are used in a variety of commercial and consumer products, including TSCA uses,
- leading to exposures of humans (<u>U.S. EPA, 2022</u>). Therefore, the relevant human routes of exposure are
- dermal, oral, and inhalation, which were the routes of exposure evaluated in a global health risk
- assessment for D4 (Gentry et al., 2017).

124

- There are limited experimental data on D4 exposure in humans. Physiologically-based pharmacokinetic (PBPK) models represent an essential tool to fill these knowledge gaps for risk assessment purposes,
- informing internal dose metrics based on exposure. The most recently published D4 PBPK model
- 128 (Campbell et al., 2023) allows for route-to-route and interspecies extrapolation of the point of departure
- 129 (POD) and POD extrapolation for lifetime continuous exposures in humans. The model was developed
- using toxicokinetic data measured in male and female adult Fischer 344 (F344) and Sprague-Dawley
- 131 (SD) rats and humans and parameterized for those species, and it was adapted to address deficiencies in
- previous models that failed to accurately predict blood and fat D4 levels after longer exposures. The key
- model adaptations compared with previous iterations (<u>Campbell et al., 2017</u>; <u>McMullin et al., 2016</u>)
- were (1) conversion of the mobile lipoprotein pool (MLP) from unidirectional distribution (one-way
- liver to fat) to a recirculating, bidirectional pool between liver and fat to account for experimental data;
- 136 (2) adjustment of parameters to account for differential toxicokinetic data by rat strain; and (3)
- introduction of a parallelogram approach for MLP parameters between rat and human to account for the
- lack of long-term clearance data in humans. Together these adaptations model rat D4 plasma and fat
- 139 concentrations from inhalation exposure in rats (Campbell et al. (2023) and reproduced in Figure 4-1
- below) and humans (Figure 4-3 below) with good representation of the underlying experimental data.
- The model predicts D4 concentrations in plasma and exhaled breath from dermal exposures for one
- human experimental dataset with acceptable accuracy (Campbell et al. (2023) and reproduced in Figure
- 4-3 below). However, it underpredicts the concentrations in exhaled breath for another human dermal
- 145 4-3 below). However, it underpredicts the concentrations in exhaled breath for another number definal
- experimental dataset (see Figure 4-4). The model also accurately predicts the concentration in plasma
- 145 for oral exposure in humans (Figure 4-5). The model does is not parameterized for dermal absorption in
- 146 rats.

- In summary, the selected model is a result of continuous refinements to PBPK models that have been
- developed over the past two decades to understand kinetics of D4 absorption in body tissues in humans
- and laboratory animals. Compared with previous versions, the current version offers the most accurate
- simulation of measured D4 concentrations in plasma, liver, and fat, even for postexposure time periods.
- The model is applicable to oral, inhalation, and dermal routes of exposure in humans. Therefore, it
- allows for rapid risk assessment of D4 for exposure scenarios in which experimental or read-across data
- are not available.

1 BACKGROUND INFORMATION

1.1 Physicochemical Properties

The physicochemical properties of D4 were summarized by EPA (U.S. EPA, 2022). D4 is a low molecular weight (296.61 g/mol), highly lipophilic substance with a log octanol:water partition coefficient (log K_{OW}) of between 6.59 at 5.7 °C and 7.13 at 34.8 °C (U.S. EPA, 2022; Xu and Kropscott, 2014, 2012). It is predicted to be highly volatile with a low boiling point of 175 °C (O'Neil et al., 2013), vapor pressure of 1.05 mm Hg at 25 °C (Flaningam, 1986) and Henry's Law constants ranging from 1.4 at 5.7 °C to 31.1 at 34.8 °C atm·m³/mol (Xu and Kropscott, 2012). Its melting point is 17.5 °C (O'Neil et al., 2013), and its density is 0.95603 g/cm³ at 20 °C (Zhang et al., 2015). The viscosity at 25 °C is 2.3 cP (Butts et al., 2003).

1.2 Absorption, Distribution, Metabolism, and Excretion (ADME) and Pharmacodynamic Considerations

Absorption

Consistent with the highly lipophilic and volatile nature of D4, absorption has been documented by the dermal and inhalation routes in humans and by the oral, dermal, and inhalation routes in rats and other species (reviewed in Brooke et al. (2009)). Approximately 5 percent of the inhaled dose is absorbed in animals, whereas between 6 to 17 percent is absorbed in humans. Consistent with the highly volatile nature of D4, absorption by the dermal route is very low, representing 0.5 to 1.1 percent of the applied dose in both rats and humans (Brooke et al., 2009; Jovanovic et al., 2008; Reddy et al., 2007; Dow Corning, 2001b; University of Rochester Medical Center, 2000). The highest absorption rates in rats are by the oral route and are vehicle dependent (Brooke et al., 2009; Dow Corning, 1998b). In a recent study in which Fischer 344 rats were administered 30 mg ¹⁴C-D4/kg bw by oral gavage in a liquid diet dosing solution, the mean percentage of the administered dose absorbed was 77.2 and 72.5 percent in female and male rats, respectively (Domoradzki et al., 2017).

Distribution

Following oral absorption after single oral gavage administration of 14 C-D4 at 30 mg/kg bw to female and male Fischer 344 rats, D4 was distributed widely throughout the body, including in blood, perirenal fat, liver, lungs, adrenals, the digestive tract, spleen, uterus, ovaries, and testes ($\underline{\text{Domoradzki et al.}}$, 2017). Peak concentration (C_{max}) values were observed two hours post-dosing in all tissues except fat, wherein C_{max} was observed 12 hours after oral gavage. The highest levels were observed two hours after exposure in the adrenals and digestive tract.

Distribution to blood, liver, lung, testes, and ovaries were also observed in seven studies after single and repeated inhalation exposures in rats, with delayed accumulation in fat (reviewed in Franzen et al. (2017)]. C_{max} values varied by study design, and the highest C_{max} values were most often observed in fat after both single and repeated exposures. In two of the studies in Fischer 344 rats exposed through a 6 hour inhalation exposure to ¹⁴C-D4 (700 ppm), D4 was widely distributed with the highest concentrations measured in fat and the lowest concentrations in the eye, spleen, and muscle (Bio-Research Laboratories LTD, 1996a, b). Radioactivity was recovered in all tissues measured, including blood, liver, lungs, nasal mucosa, larynx, trachea, kidney, adrenals, heart, brain, spleen, pancreas, thymus, eyes, testes, vagina, uterus, ovaries, bone, muscle, skin, fat, stomach, small intestine, and large intestine (Bio-Research Laboratories LTD, 1996a, b).

Similar widespread tissue distribution patterns after inhalation exposure were also observed in an additional study in which Fischer 344 rats exposed to ¹⁴C-D4 at 7 or 700 ppm for 6 hours per day for 14 days (ClinTrials, 1997). Peak blood, plasma, and tissue radioactivity levels were reached between 0 and 3 hours after the end of each exposure, and high levels persisted in fat tissues through 168 hours. High levels of D4 were found in the respiratory tract, liver, and thymus. The highest levels of D4 were measured in adrenals, nasal mucosa, and fat, and lower levels were measured in reproductive tissues. With the exception of adrenal glands in which C_{max} and area under curve (AUC) levels were higher in females compared with males, there were no significant differences in tissue distribution by sex.

Although studies examining D4 distribution in humans are lacking, oral and inhalation exposure studies in rodents indicate a very widespread distribution of D4 across tissues and matrices. It should be noted, however, that definitive studies directly comparing distribution across tissues and matrices by route in animals were not identified. Furthermore, modeling studies indicate D4 entry to blood varies by route of exposure (Sarangapani et al., 2003). After oral exposure, D4 enters the deep blood compartment within the triglyceride core in chylomicrons via the lymphatic system, and transport of D4 from the deep blood compartment to fat compartments provided the best fits to observed plasma, urine, and exhaled D4. Entry to blood via dermal and inhalation routes would bypass this process, which is consistent with pharmacokinetic (PK) modeling work by Centre Européen des Silicones (CES, 2005), as reviewed in Brooke et al. (2009), suggesting that oral D4 is absorbed by chylomicrons or other lipoproteins that may be removed from the blood in the liver, leaving a lower proportion of the absorbed dose available for systemic distribution compared with that from inhalation exposure.

Metabolism

After absorption, D4 metabolism is thought to occur primarily in the liver. Specific urinary metabolites were identified in rats administered radiolabeled D4 via the intravenous (IV) route by Varaprath et al. (1999). While no parent D4 was identified in urine, two major and five minor metabolites were identified. The major metabolites were identified as dimethylsilanediol [Me2Si(OH)2] and methylsilanetriol [MeSi(OH)3] and constituted 75 to 85 percent of the total radioactivity. Minor metabolites were identified as tetramethyldisiloxane-1,3-diol [Me2Si(OH)-O-Si(OH)Me2], hexamethyltrisiloxane-1,5-diol [Me2Si(OH)-OSiMe2-OSi(OH)Me2], trimethyldisiloxane-1,3,3-triol [MeSi(OH)2-O-Si(OH)Me2], dimethyldisiloxane-1,1,3,3-tetrol [MeSi(OH)2-O-Si(OH)2Me], and dimethyldisiloxane-1,1,1,3,3-pentol [Si(OH)3-O-Si(OH)2Me]. The proposed metabolic pathway based on identification of these metabolites is an initial oxidation of methyl groups by cytochrome P450 (CYP P450) enzymes and subsequent rearrangement and hydrolysis to generate the major metabolites (citing Varaprath et al. (1999) and reviewed in Andersen (2022)) Further hydrolysis and oxidation generate linear silanol minor metabolites. Studies in humans indicated that the parent compound is rapidly cleared followed by slower clearance of metabolites with half-lives of several days (citing Reddy et al. (2003) and reviewed in Andersen (2022)).

Excretion

Excretion of D4 is primarily through urine and then exhaled air and feces. While elimination is observed on the order of minutes after exposure, persistence of D4 after cessation of exposure suggests that D4 in blood exists in two pools: free D4 available for excretion via exhalation and a reservoir of D4 that is likely packaged into blood lipids and lipoproteins and thus is less available for excretion (Campbell et al., 2017; Andersen et al., 2001).

The half-lives of radioactivity were measured after acute nose-only inhalation exposure for 6 hours to 7, 70 or 700 ppm ¹⁴C-D4 mixed with unlabeled D4 in Fisher 344 rats. The half-life in plasma, skin, and testes were 68, 154, and 273 hours, respectively (Bio-Research Laboratories LTD, 1996b), and were

consistent with those reported by Plotzke et al. (2000) in a study using the same exposure paradigm. In addition to testes and skin, long half-lives were measured in lung, nasal mucosa, fat, eye, uterus, and vagina. Elimination after the nose-only 6 hour exposure appeared multiphasic in blood, plasma, and most organs in that a rapid decline was observed over the first 24 hours postexposure followed by a long, terminal elimination phase. In an oral dosing study in rats administered 30 mg [¹⁴C] D4/kg bw, the fastest terminal half-lives were in blood (20 hours in females and 18.7 hours in males) (Domoradzki et al., 2017). The slowest terminal half-lives were in perirenal fat (233.6 hours) and ovaries (246.7 hours) in females and in perirenal fat (166.8 hours) and spleen (87.7 hours) in males. In this study, radioactivity was detected in feces, expired volatiles, and urine through the entire 168 hour observation period. However, the highest concentrations of radiolabel were measured in expired volatiles during early (1–2 and 2–4 hour) collection periods, in urine during the 12 to 24 hour collection period, and in feces during the 0 to 24 hour collection period. The recovered doses ranged from 32 to 40 percent in urine, 18 to 30 percent in expired volatiles, and 22 to 27 percent in feces with sex impacting the variability. Thus, D4 half-lives are relatively short (hours to days).

Similar excretion patterns were observed after repeat-dose inhalation exposure to ¹⁴C-D4 in rats (ClinTrials, 1997) for 14 days. The elimination profile in blood was multiphasic with a rapid initial decline in the first 24 hours followed by a long terminal elimination phase, which was reflected by the wide range of half-lives measured (56–253 hours). Highest half-life values were measured in lung, testes, nasal mucosa, and fat, and the shortest half-life was measured in plasma. Elimination was primarily through renal and pulmonary routes and was impacted by the dose. Radioactivity in excreta was highest in urine (37–40%) and expired volatiles (25%), followed by feces (12–19%) and expired ¹⁴CO₂ (2–5%). There were no sex-specific differences in recovery from excreta.

D4 exhibits some unique toxicokinetic characteristics compared with other highly lipophilic volatile organic compounds. For example, the lower than expected portioning from blood to air along with the higher than expected fat:blood partitioning suggested a pool of D4 in blood that was associated with lipids and thus not available for exhalation (Campbell et al., 2017; Andersen et al., 2001). These observations support a distribution model in which D4 is incorporated into lipid storage compartments that are not in equilibrium with free D4 in blood (Andersen et al., 2001). In addition, D4 exhibits high metabolic clearance rates that may reflect the ability of D4 to induce hepatic metabolic enzymes in a manner similar to phenobarbital. Consistent with the toxicokinetic characteristics described above, these observations suggest a slow release of D4 from fat compartments and D4 binding to a lipoprotein compartment in blood called a mobile lipid pool (MLP). Several published PBPK models account for D4 toxicokinetic profile through integrating an MLP parameter (Campbell et al., 2017; McMullin et al., 2016; Sarangapani et al., 2003; Andersen et al., 2001). EPA selected the most recent adaptation of this model that captures the toxicokinetic characteristics of D4 and accurately predicts human concentrations after long-term exposures (Campbell et al., 2023).

1.3 Toxicity of D4

1.3.1 Summary of D4 Toxicity in Humans

At least one study in humans acutely exposed to D4 via inhalation showed no effects on lung function (forced vital capacity [FVC] and forced expiratory capacity [FEV1]) when exposed to 10 ppm (121.3 mg/m3) of D4 vapor for 1 hour (<u>Utell et al., 1998</u>). A second study in which subjects were exposed orally to 12 mg/day of D4 for 14 days found no immunotoxic or pro-inflammatory adjuvant effect (<u>Dow Corning, 1998a</u>). The potential for effects on the immune system was inferred by a study of human peripheral blood mononuclear cells (PBMC) exposed to D4 in vitro. At D4 concentrations greater than

 $10 \,\mu\text{M/mL}$, phytohemagglutinin-mediated proliferation was inhibited under culture conditions without serum. However, because this effect was attenuated by presence of serum, the potential relevance to human exposures in vivo is unclear (citing University of Rochester Medical Center (2002), and reviewed in Franzen et al. (2017)). No chronic exposure studies in humans were identified.

1.3.2 Summary of D4 Toxicity in Animals

Acute Exposure

295

296

297

298

299

300 301

302

303

304

305

306

307

308 309

310 311

312

313

314

315

316

317318

319

320

321 322

323

324

325

326

327

328329

330

331

332

333

334

335

336

337

338

339 340

341

342

Exposure to D4 after acute exposure by oral, dermal, and inhalation routes of exposure showed little toxicity in rats and mice. For example, in Wistar rats, the oral lethal dose (LD) 50 was estimated to be greater than 4,800 mg/kg bw, and the dermal LD50 was estimated to be greater than 2,400 mg/kw bw (reviewed in Franzen et al. 2017) and Brooke et al. (2009)). In CD-1 mice, the LD50 was 1,700 mg/kg by the oral route as reviewed in Franzen et al. (2017) and 6,000 to 7,000 mg/kg by the intraperitoneal (IP) route (Lieberman et al., 1999). In F344 rats, the inhalation lethal concentration (LC)50 was estimated to be 36 mg/L (3,600 mg/m³) after a single 4-hour exposure (Dow Corning, 1994). In this study, a subset of animals of both sexes exposed to the higher doses (30–54 mg/L) exhibited tachypnea.

Repeated Exposures

In repeated (14 day) oral gavage studies in Sprague-Dawley (SD) rats, a no observed acute exposure level (NOAEL) of 25 mg/kg/day was derived for liver toxicity measured as liver enlargement and increased liver weight associated with elevated CYP2B1/2 levels (citing Dow Corning (1990) and reviewed in Brooke et al. (2009)). D4 was not associated with skin sensitivity in humans or skin and eye sensitivity in rabbits and guinea pigs, as reviewed in Brooke et al. (2009) and Franzen et al. (2017).

Repeated-dose inhalation studies found that after a 5-day exposure study in rats, the lowest-observedeffect concentration (LOEC) was 85 mg/m³ (7–10 ppm) and was associated with liver toxicity including phenobarbital-like increased hepatic CYP2B1/2 enzyme levels and liver cell proliferation measured as proliferating cell nuclear antigen (PCNA) expression and bromodeoxyuridine (BrdU) incorporation into hepatic DNA (Meeks et al., 2022; Dow Corning, 2001a; McKim et al., 2001a; McKim et al., 1998). At higher concentrations, other organs exhibited signs of toxicity measured as increased liver, thyroid, lung, uterus, ovary, pituitary, and adrenal weights and decreased thymus weights (citing Dow Corning (2002, 2001a) and reviewed in EC/HC (2008)). In a two-year inhalation studies in rats, alveolar sub-pleural chronic inflammation in the respiratory tract was observed at doses as low as 10 ppm in females (Dow Corning, 2004). In this and another study, histopathological changes were observed as early as 12 months in mice exposed to 700 ppm (8492 mg/m³) including hyperplasia of nasal cavity squamous epithelial cells and goblet cells in both sexes (Dow Corning, 2004). In a three-month repeated dose inhalation study (6 hours/day for 5 days/week) using concentrations of 0.3 and 12.0 mg/L (300–12,000 mg/m³), histopathological analysis noted a dose-dependent increase in the incidence of chronic interstitial inflammation in the lung (RCC, 1995). Increased liver weights were also observed in mice and hamsters in 28-day and 35-day inhalation studies but not in rabbits or guinea pigs (citing Dow Corning (2001c), and reviewed in SCCS (2010)). In rats, increased liver weights correlated with increased hepatocyte proliferation in males and females after inhalation exposure to 700 ppm for 5 days (Dow Corning, 2001c). Liver weights were also not increased in rabbits exposed to doses of up to 1,000 mg/kg/day for 14 days, suggesting that D4 exerts species-specific toxicity (citing Dow Corning (2001c), and reviewed in Brooke et al. (2009) and SCCS (2010)).

In addition to effects in liver, lung, and other organs, repeat dosing studies revealed that D4 impacts fertility and reproduction in rats). Uterine weight was significantly increased in female rats administered 250 mg/kg/day D4 and higher by gavage in both Fischer 344 and Sprague-Dawley rats (MPI Research,

1999). Decreased numbers of implantation sites, decreased corpora lutea, increased pre-implantation loss, and reduced mean live litter size were observed in studies in female rats exposed to 700 ppm for 6 hours per day from 28 days prior to mating through gestation day (GD) 20 (Meeks et al., 2007). A more detailed analysis in this study (Meeks et al., 2007) examined effects after exposure during specific phases of the reproductive cycle that included an overall phase, ovarian phase, fertilization phase, and implantation phase. Female rats were exposed to various concentrations up to 700 ppm daily during the selected phases for 6 hours per day. In animals exposed to <300 ppm during the overall phase (28 days prior to mating through GD19), the number of corpora lutea, implantation sites, and offspring were significantly decreased. No significant changes were reported in the ovarian and implantation phases. However, when females were exposed in the fertilization phase (3 days prior to mating to GD3), uterine implantation and post-implantation losses were observed and the number of corpora lutea decreased at the 700-ppm exposure dose. Additional studies in this report indicated that exposure to D4 in the premating phase was the most critical period impacting the reproductive effects of D4.

Subchronic and Chronic Exposure

A three-month inhalation study in rats derived an LOEC of 420 mg/m³ based on increased liver and adrenal weights, decreased thymus weights, and inflammatory changes in lungs of both sexes (RCC, 1995). In a two-year inhalation study in rats using a 700 ppm exposure dose, toxicity in multiple organ systems was observed that included altered clinical chemistry results for multiple enzymes and total protein, lymphocytic leukocytosis, hepatocellular hypertrophy and increased liver weights, chronic nephropathy and increased kidney weights, increased testis weights, increased uterine weights and a non-significant increase in uterine benign endometrial adenomas, and a statistically significant increase in the incidence of uterine endometrial epithelial hyperplasia (Jean and Plotzke, 2017).

Mechanisms of Toxicity

Generally, the mechanisms by which D4 exposure mediates health effects are not well understood. Furthermore, no studies were identified that differentiated the toxic effects of the parent D4 and its metabolites in humans or animals (reviewed in Franzen et al. (2017)). Therefore, it is not known whether the toxic effects described in humans or animals require metabolism of the parent compound.

For the parent D4, tests of mutagenicity and DNA damage were uniformly negative in vitro (prokaryotic and eukaryotic cells) and in vivo (reviewed in Brooke et al. (2009), ECHA (2016), EC/HC (2008), and Franzen et al. (2017)). Other proposed mechanisms or modes of action relate to activation of nuclear xenobiotic sensing receptors and disruption of hormone signaling. Given the similarities between D4 and PB, liver enlargement and hepatic CYP induction is postulated to manifest, at least in part, through activation of the constitutive androstane receptor (CAR) (Andersen, 2022; CIIT, 2005). Using a human hepatocarcinoma cell line (HepG2) reporter assay, D4 activated both human and rat CAR at a concentration of 62.5 μ M, and human CAR was more sensitive to D4 than rat CAR (CIIT, 2005). D4 has also been shown to activate the pregnane X receptor in an in vitro reporter gene assay at concentrations of 31 μ M and greater (Dow Corning, 2005).

In addition, there is evidence of altered hormone function and signaling as a mechanism of D4-mediated pathogenetic effects. In particular, the effects on fertility and reproduction may, at least in part, derive from the ability of D4 to interfere with the preovulatory luteinizing hormone (LH) surge that precedes and is required for the meiotic maturation of eggs and ovulation. After inhalation exposure to 700 ppm D4 (6 hours/day for 3 days), female rats exhibited reduced peak proestrus LH concentrations, and on the day of ovulation, estradiol levels were increased and follicle stimulating hormone (FSH) levels decreased (Quinn et al., 2007a). These hormonal changes were associated with 47 percent fewer rats ovulating compared with controls. The precise mechanism does not appear to be related to weak

estrogenic and anti-estrogenic activities described for D4 (Quinn et al., 2007b; McKim et al., 2001b) despite the observation that pretreatment of mice with an estrogen receptor antagonist precludes D4-mediated uterotrophic effects including increased uterine weights (Dow Corning, 2001c) (reviewed as Dow Corning (1999) in SCCS (2010)). Rather, three alternative mechanisms have been proposed (Quinn et al., 2007a). Given the similarities in suppressing the LH between D4 and barbiturates such as phenobarbital (PB), D4 may act in a similar fashion to PB by disrupting hypothalamic norepinephrine neurotransmission during a key period of the hypothalamic pituitary ovarian axis regulation. A second hypothesis is that D4 acts as an indirect dopamine agonist that results in attenuation of the prolactin peak that precedes the LH surge. A third possibility is that D4 may alter transport or release gonadotropin-releasing hormone (GnRH) that functions to stimulate LH release in the pituitary gland, possibly through blocking norepinephrine signaling required for GnRH release.

Establishing the mechanism of D4 disruption of LH release is critical to making inferences for potential D4 effects on human fertility and reproduction. Whether observations in rodent-related LH suppression extrapolates to humans is questionable because the human LH surge is regulated through different processes. For example, unlike in rodents, the human LH surge is not subjected to the environmental cues and timing restrictions observed in rodents. More specifically, in rodents, the LH surge initiates with the release of GnRH by a neural signal that is coupled to the light-dark cycle of estradiol in the preoptic area (POA). In humans, control of the LH surge is through the mediobasal hypothalamus (MBH) leading to LH stimulation in pituitary gland. Furthermore, the relatively weak affinity of D4 for the estrogen and progesterone receptors argue against D4 estrogenic activity for the endometrial proliferative lesions observed in the two-year study. Further studies are required to delineate the precise mechanism in rodents and implications for human reproduction and fertility.

1.4 Regulatory History of D4

Several government agencies have conducted reviews or risk assessments for D4. In 2008, Environment Canada/Health Canada (EC/HC, 2008) concluded that while D4 is entering or may be entering the environment in a quantity or concentration or under conditions that may have an immediate or long-term harmful effect on the environment or its biological diversity, it is not entering the environment in a quantity or concentration that may constitute a danger to human life or health. Health Canada was unable to decide whether D4 should be subjected to its Persistence and Bioaccumulation Regulations (EC/HC, 2008). In 2009, the United Kingdom's Environmental Agency conducted an environmental risk assessment of D4 (Brooke et al., 2009). This agency concluded that there are also no risks for humans exposed to D4 via the environment; however, due to uncertainties, it could not make definitive conclusions regarding other environmental risks. In 2016, the European Chemicals Agency's Committee for Risk Assessment (RAC) and Committee for Socio-economic Analysis (SEAC) determined that D4 meets the definition of a persistent, bioaccumulative, and toxic (PBT) substance and a very persistent, very bioaccumulative (vPvB) substance according to Annex XIII of the European Union (EU) regulation on the registration, evaluation, authorization and restriction of chemicals (REACH) (ECHA, 2016; Brooke et al., 2009). ECHA recommended relevant uses result in total EU releases to wastewater of approximately less than 20 tons per year. Under Annex VI, D4 was assigned a Hazard Class and Category Code designation of Repr. 2 (H361f: Suspected of damaging fertility) and an Aquatic Chronic designation of Aquatic Chronic 4 (H413: May cause long lasting harmful effects to aquatic life). In 2020, the American Chemistry Council's Silicones Environmental, Health, and Safety Center (SEHSC), on behalf of several manufacturers, requested that EPA conduct a risk evaluation for D4 (Docket ID: EPA-HQ-OPPT-2018-0443). The Agency granted the request on October 6, 2020, and published the Final Scope of the Risk Evaluation for Octamethylcyclotetrasiloxane (Cyclotetrasiloxane, 2,2,4,4,6,6,8,8-octamethyl-) (D4); CASRN 556-67-2 in February 2022 (U.S. EPA, 2022). In furtherance of EPA's risk evaluation for D4, EPA evaluated suitable PBPK models to establish route-to-route and

interspecies extrapolation of the point of departure (POD) and POD extrapolation for lifetime continuous exposures in humans.

1.5 D4 PBPK Models

The first efforts at modeling D4 exposure started in the early 2000s, using data from an inhalation kinetic study in rats (Andersen et al., 2001). That study revealed low blood: air and high fat:blood partitioning, high metabolic clearance, and slower clearance from tissues than expected (McMullin et al., 2016; Andersen et al., 2001). In addition, as noted by McMullin, "a discrepancy between the rate of D4 elimination via exhalation and the associated blood levels following inhalation exposure indicated the presence of a pool of D4 in the plasma that was not available for exhalation." To account for such data, deep-tissue compartments were introduced to predict slow loss of D4 after the exposure. In addition, McMullin et al. (2016) adapted the model to account for a pool or compartment in blood assumed to represent lipoproteins (the MLP) and multiple fat compartments to describe slower release of D4 from fat compartments and longer time frames for exhalation curves. The model was later expanded to include oral and dermal exposure routes (Sarangapani et al., 2003). With availability of data for humans, the model was further developed to include inhalation and dermal exposure in humans (Reddy et al., 2007). McMullin et al. (2016) integrated all the models available by that time into a multi-route model for rats and humans. Later, new experiments provided time-series data from oral bolus administration in rats (Domoradzki et al., 2017). However, McMullin's model was limited to accurately predicting the rate of the D4 exchange in exhaled breath, plasma, liver, and fat. Campbell and colleagues made refinements to the model for more accurate simulation of the metabolism in the liver. The refined model had a better agreement with rat oral data. The current version of the model is a result of further refinements to the Campbell 2017 model. The most important one is the replacement of singledirectional MLP compartment with a bidirectional compartment to reproduce extended clearance data of D4 from blood and fat. This refinement allows for simulation of a 28-day D4 inhalation exposure time, as well as a 14-day postexposure time in male and female F344 and SD rats. Another refinement was to consider the differences in D4 metabolism in the liver in the SD and F344 rats by tuning metabolic parameters. Finally, they introduced a parallelogram approach to parameterize MLP from the ratio of the human to rat parameters.

1.6 Model Data

In the current version of the model, the most recent rat inhalation data were used (Meeks et al., 2022) because this was the most recent data that measured D4 concentrations across multiple tissues, matrices and time points in both the exposure and post-exposure periods in two different rat strains (F344 and SD) exposed to 700 ppm D4. Additional recent datasets (Schmitt et al., 2023) were included because multiple dose levels were examined in F344 and SD rats (7, 70, and 700 ppm along with concentration measurements over time for multiple tissues and matrices). The human inhalation exposure data (Utell et al., 1998) used in previous models were also used in the current model to allow for comparison between different models. The model was also applied to data from the only human dermal study (Plotzke et al. (2000) as cited in Reddy et al. (2007)) with significant amounts of D4 in exhaled breath and plasma after a single-time exposure (Campbell et al., 2023; Campbell et al., 2017).

478 479 480

481

482

483

484

485

486

442443

444

445 446

447

448

449

450

451

452

453

454

455

456

457

458

459

460

461

462

463

464 465

466

467

468 469

470

471 472

473 474

475

476

477

There are D4 toxicokinetic studies in rats and humans that are not used in construction or validation of the current model. Examples are in vivo dermal studies in rats that lack concentration data over time for important compartments such as plasma and fat (<u>Dobrev et al., 2008</u>; <u>Jovanovic et al., 2008</u>). The same is true for chronic studies in F344 rats (<u>Jean and Plotzke, 2017</u>). Such data are required for appropriate modeling. A human dermal study conducted by Biesterbos et al. (<u>2015</u>) found insignificant amounts of D4 in exhaled breath. They concluded that dermal absorption provides a negligible contribution to the internal dose, and inhalation must be considered as the main route for risk assessment.

487
488

489

490

491

492493

Another notable dermal study was conducted by Jovanovic et al. (2008) in rats. Although the study did provide the time course of D4 in blood, D4 concentrations were below detectable levels. The study did report detectable levels in expired volatiles, urine, and feces were reported for 1, 6, 24, and 168 hours after a single dose administration. Other data from human studies were excluded, such as the analysis of methylsiloxanes in plasma of pregnant and postmenopausal women (Hanssen et al., 2013) or children (Guo et al., 2021), due to unknown exposure levels or unclear exposure routes.

2 MODEL PURPOSE

The model was developed by Campbell et al. (2023) to provide insight into kinetic parameters of D4
exposure in rats through oral and inhalation routes and in humans through inhalation and dermal routes.
Compared with similar PBPK models, the current one offers more accurate simulation of clearance data
for longer time periods and accounts for rat strain differences in metabolism of D4. Importantly, the
human D4 model provides good fits to the human exposure studies. Therefore, this model was deemed
the most appropriate for risk assessment applications of D4.

501 3 MATERIALS AND METHODS

3.1 Modeling Strategy

The strategy for developing the current model was to 1) convert the unidirectional MLP into a bidirectional pool between liver and fat (Figure 3-1) to surpass the shortcomings of the previous models in predicting kinetic data in rats and 2) revise the liver metabolism to account for differences in rat strains.

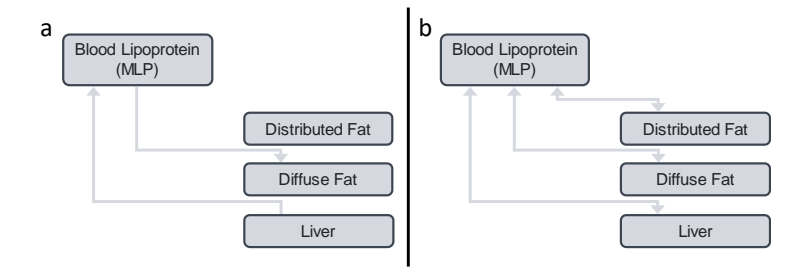


Figure 3-1. Conversion of MLP from (a) Unidirectional to (b) Bidirectional Compartment Figure is adapted from <u>Campbell et al. (2017)</u> and <u>Campbell et al. (2023)</u>. Gray arrows indicate directionality of MLP and fat compartments introduced in the model.

The current version also was adapted to a contemporary interface. The older version of the model was written in acslX and has been translated into R using MCSim (version 6.0.1) and RTools (version 3.5.0.4) in the current version.

3.2 Summary of Data for Model Development and Evaluation

Model Data

The current model (Campbell et al., 2023) is based on data from inhalation, oral, and dermal exposure in rats and inhalation and dermal exposure in humans summarized by Campbell et al. (2017). D4 concentration data for F344 rats were obtained from plasma, peripheral fat, lung, liver, urine, and feces. In humans, D4 amounts were measured in blood, exhaled breath, and urine of the subjects during exposure to ¹⁴C-D4 vapor while performing physical exercises or a single-time application of 1–1.4 g of ¹³C-D4 to skin axilla (Plotzke et al. (2000) as cited in Reddy et al. (2007)). Metabolism of D4 occurs in the liver through saturable Michaelis-Menten kinetics that result in linear silanols (McMullin et al., 2016; Sarangapani et al., 2003). Empirical metabolism data applied in the model were obtained from metabolic clearance of D4 into urine and feces in rats (Plotzke et al., 2000).

Model Compartments

For inhalation and dermal routes of exposure, the model has the following compartments: arterial blood, venous blood, lung tissue, rapidly perfused tissues, slowly perfused tissues, distributed fat, diffuse fat, blood lipoprotein, liver, skin, metabolite, urine, and feces (Figure 3-2). Campbell and colleagues incorporated a revised oral uptake description to reflect the time course of parent D4 in exhaled breath and blood after oral bolus dosing. They also used allometric scaling of rate constants to preclude the requirement for sex-specific parameterization in F344 rats. The updated model also includes an oral submodel that contains stomach and duodenum (Campbell et al., 2017).

3.3 Model Development and Structure

The schematic diagram of the model is presented in Figure 3-2 and adapted from Campbell et al. (2023). The model is applicable to F344 and SD rats and humans, and accommodates inhalation, oral, and dermal routes of exposure. Physiological parameters are obtained from Brown et al. (1997), a commonly used resource for human PBPK modeling. Revised chemical-specific parameters for the current model are presented in Campbell et al. (2023; 2017). As discussed in Section 1, the model includes several deep-tissue compartments to simulate gradual postexposure loss of D4 and multiple fat compartments to "describe the longer-time exhalation curves indicative of slower release of D4 from fat compartments," as noted by McMullin et al. (2016). Campbell et al. (2017) have included "sequestered (*i.e.*, lipid associated) oral absorption into plasma after oral bolus dosing to describe the lack of exhalation as well as the initial distribution of siloxane to the liver which was higher than simple partitioning from plasma would allow."

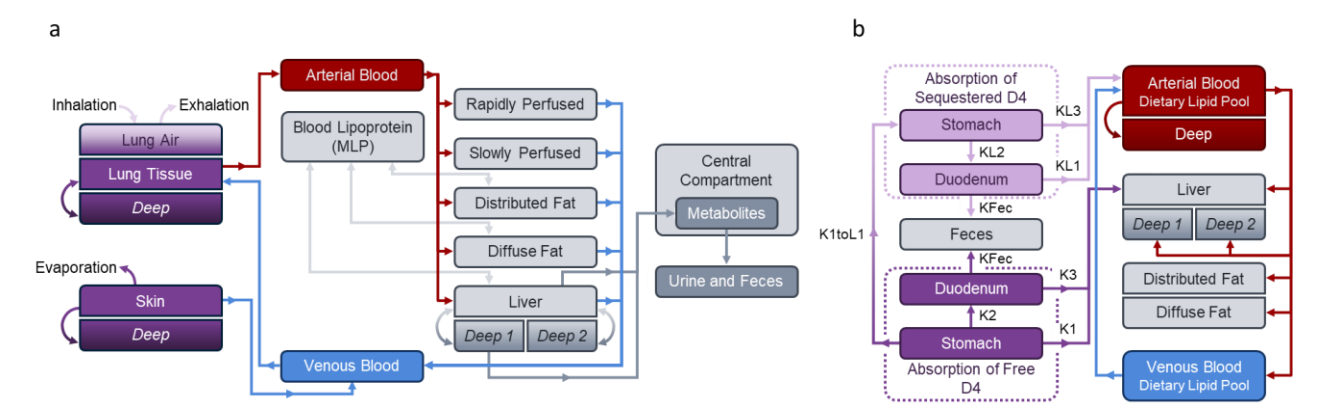


Figure 3-2. PBPK Model Diagram for Rat and Human Adapted from Campbell et al. (2023) (a) Inhalation and dermal exposure, (b) Oral submodel. K1, K2, K3, KL2, KL3, and KFec are first order rate constants for transfer between different compartments (1/hr). K1toL1 is the rate constant for conversion of free D4 to sequestered D4 (1/hr).

3.4 Model Equations

Table 3-1 lists prefixes and abbreviations used in naming parameters in the model code. The following are the main differential equations used in the model construction. Each parameter is described in the following subsection.

Table 3-1. List of Prefixes Used in the Model

Prefix	Description (units)				
A	Amount				
Q	Blood flow (L/hr/kg ^{0.75} , fraction of cardiac output)				
V	Volume (L)				
С	Concentration (mg/L)				
K	Rate constant (1/hr)				
P	Partition coefficient (unitless)				
R	Rate (mg/hr)				
RA	Rate amount				

Abbreviation	Description
ABS	Absorption
AIR	Air
ALV	Alveolar
ART	Arterial
BLD	Blood
CYP	CYP enzyme
DIFF	Diffuse fat
DIST	Distributed fat
ELIM	Elimination
FAT	Fat
FEC	Feces
INH	Inhalation
L	Lipid
LIV	Liver
LNG	Lung
MET	Metabolism
MLP	Mobile lipoprotein pool
PROD	Production
RAP	Rapidly perfused tissues
SKN	Skin
SLW	Slowly perfused tissues
TOT	Total
VEN	Venous

3.4.1 Arterial Blood

565566567

564

Equation 3-1. Amount of D4 in Blood Lipid in Arterial Blood (mg)

568569570

$$\frac{d(A_{ArtBldMLP})}{dt} = Q_C \times \left(\frac{A_{VenBldMLP}}{V_{VenBld}} - \frac{A_{ArtBldMLP}}{V_{ArtBld}}\right) - RA_{LeaveMLPF} - RA_{LeaveMLPL}$$

571 572

573

574

$$\frac{d(A_{ArtBldDLP})}{dt} = \left(Q_C \times \left(\left(\frac{A_{VenBLDDLP}}{V_{VenBld}}\right) - \left(\frac{A_{ArtBldDLP}}{V_{ArtBld}}\right)\right)\right) - K_{RemovalF} \times C_{ArtBldDLP} \times V_{ArtBld} - K_{RemovalL} \times C_{ArtBldDLP} \times V_{ArtBld} - K_{RemovalFDist} \times C_{ArtBldDLP} \times V_{ArtBld} + RO_{AbsL}$$

575576

Equation 3-3. Amount of D4 in Arterial Blood "Free" (mg)

 $A_{ArtRIdTot} = A_{ArtRId} + A_{ArtRIdMLP} + A_{ArtRIdDLP}$

$$\frac{d(A_{ArtBld})}{dt} = Q_C \times \left(CV_{Lng} - C_{ArtBld}\right)$$

582 Equation 3-4. Total Amount of D4 in Arterial Blood (mg)

3.4.2 Venous Blood

Equation 3-5. Amount of D4 in Blood Lipid in Venous Blood (mg)

$$\frac{d(A_{VenBldMLP})}{dt} = RA_{ProdMLP} + RA_{ProdMLPLDeep} + RR_{ProdMLPFDist} + RA_{ProdMLPFDiff} + \left(Q_C \times \left(\left(\frac{A_{ArtBldMLP}}{V_{ArtBld}}\right) - \left(\frac{A_{VenBldMLP}}{V_{VenBld}}\right)\right)\right)$$

Equation 3-6. Amount of D4 in Dietary Blood Lipid in Venous Blood (mg)

$$\frac{d(A_{\text{VenBldDLP}})}{dt} = \left(Q_C \times \left(\left(\frac{A_{ArtBldDLP}}{V_{ArtBld}}\right) - \left(\frac{A_{VenBldDLP}}{V_{VenBld}}\right)\right)\right)$$

Equation 3-7. Amount of D4 in venous blood (mg)

$$\frac{d(A_{VenBld})}{dt} = \left(Q_{FatDiff} \times CV_{FatDiff} + Q_{FatDist} \times CV_{FatDist} + Q_{Liv} \times CV_{Liv} + Q_{Rap} \times CV_{Rap} + \left(\frac{K_{SknBld} \times Derm_{Area1} \times A_{Skin1}}{Derm_{Area1} + 1.0e - 23}\right) + \left(\frac{K_{SknBld} \times Derm_{Area2} \times A_{Skin2}}{Derm_{Area2} + 1.0e - 23}\right) + Q_{Slw} \times CV_{Slw}\right) - \left(Q_C \times C_{VenBld}\right)$$

Equation 3-8. Total Amount of D4 in Venous Blood Compartment (mg)

$$A_{VenBldTot} = A_{VenBld} + A_{VenBldMLP} + A_{VenBldDLP}$$

3.4.3 Lung

Equation 3-9. Amount of D4 in 1st Deep Lung Compartment (mg)

$$\frac{d(A_{LngDeep1})}{dt} = \left(K_{LngDeep1In} \times V_{Lng} \times \left(\frac{A_{Lng}}{V_{Lng}}\right)\right) - \left(K_{LngDeep1Out} \times V_{Lng} \times \left(\frac{A_{LngDeep1}}{V_{Lng}}\right)\right)$$

613
$$\frac{d(A_{Lng})}{dt} = (Q_P \times C_{Inh}) - (Q_P \times C_{Alv}) + \left(Q_C \times \left(C_{VenBld} - CV_{Lng}\right)\right) + \left(K_{LngDeep1Out} \times V_{Lng} \times \left(\frac{A_{LngDeep1}}{V_{Lng}}\right)\right)$$
614
$$-\left(K_{LngDeep1In} \times V_{Lng} \times \left(\frac{A_{Lng}}{V_{Lng}}\right)\right)$$

3.4.4 Fat

618 Equation 3-11. Amount of D4 in Diffuse Fat (mg)

620
$$\frac{d(A_{FatDiff})}{dt} = \left(Perm_{FatDiff} \times Q_{FatDiff} \times \left(C_{ArtBld} - \left(\frac{C_{FatDiff}}{P_{FatDiff}}\right)\right)\right) + RA_{LeaveDLPF} + RA_{LeaveMLPF} \times \left(\frac{V_{FatDiff}}{V_{FatDiff}} + V_{FatDist}\right) - RA_{ProdMLPFDiff}$$

Equation 3-12. Amount of D4 in Distributed Fat (mg)

$$\begin{split} \frac{d(A_{FatDist})}{dt} &= Perm_{FatDist} \times Q_{FatDist} \times \left(C_{ArtBld} - \left(\frac{C_{FatDist}}{P_{FatDist}}\right)\right) + RA_{LeaveDLPFDist} \\ &+ RA_{LeaveMLPF} \times \left(\frac{V_{FatDist}}{V_{FatDiff} + V_{FatDist}}\right) - RA_{ProdMLPFDist} \end{split}$$

3.4.5 Liver

Equation 3-13. Induction of Metabolism in Liver by D4

$$\frac{d(A_{CYP})}{dt} = K_0 + K_{Max} \times \left(\frac{\left(CV_{Liv} + CV_{LivDeep1}\right)}{\left(CV_{Liv} + CV_{LivDeep1}\right) + K_{DLiv}}\right) - \left(K_{ElimCYP} \times A_{CYP}\right)$$

Equation 3-14. Amount of D4 Metabolized in Liver (mg)

$$\frac{d(A_{Met})}{dt} = Factor \times V_{Max} \times \frac{CV_{Liv}}{K_{M} \times \left(1 + \frac{CV_{LivDeep1}}{K_{M}}\right) + CV_{Liv}}$$

Equation 3-15

640
$$\frac{d(A_{Met2})}{dt} = \frac{Factor \times V_{Max} \times CV_{LivDeep1}}{K_M \times \left(1 + \frac{CV_{Liv}}{K_M} + CV_{LivDeep1}\right)}$$

Equation 3-16. Amount of D4 in 1st Deep Liver Compartment (mg)

644
$$\frac{d(A_{LivDeep1})}{dt} = \left(K_{LivDeep1In} \times C_{Liv} \times V_{Liv}\right) + RA_{LeaveDLPL} \times Frac_{OLDeep1} - RA_{ProdMLPLDeep}$$
645
$$-\left(K_{LivDeep1Out} \times V_{Liv} \times \left(\frac{A_{LivDeep1}}{V_{Liv}}\right)\right) - RA_{Met2}$$

Equation 3-17. Amount of D4 in 2nd Deep Liver Compartment (mg)

649
$$\frac{d(A_{LivDeep2})}{dt} = \left(K_{LivDeep2In} \times C_{Liv} \times V_{Liv}\right) - \left(K_{LivDeep2Out} \times V_{Liv} \times \left(\frac{A_{LivDeep2}}{V_{Liv}}\right)\right) + RA_{LeaveDLPL} \times Frac_{OLDeep2}$$

Equation 3-18. Amount of D4 in Liver (mg)

655
$$\frac{d(A_{Liv})}{dt} = \left(Q_{Liv} \times (C_{ArtBld} - CV_{Liv})\right) + \left(K_{LivDeep1Out} \times V_{Liv} \times \left(\frac{A_{LivDeep1}}{V_{Liv}}\right)\right) + \left(K_{LivDeep2Out} \times V_{Liv} \times \left(\frac{A_{Livdeep2}}{V_{Liv}}\right)\right) - \left(K_{LivDeep2In} \times C_{Liv} \times V_{Liv}\right) - \left(K_{LivDeep2In} \times C_{Liv} \times V_{Liv}\right) - \left(K_{LivDeep2In} \times C_{Liv} \times V_{Liv}\right) - RA_{ProdMLPL} + RA_{LeaveMLPL} + RA_{LeaveDLPL} \times \left(1 - Frac_{OLDeep1} - Frac_{OLDeep2}\right) - RA_{Met} + R_{OAbs}$$

3.4.6 Rapidly Perfused Tissues

Equation 3-19. Amount of D4 in Rapidly Perfused Tissues (mg)

Equation 3-20. Amount of D4 in Slowly Perfused Tissues (mg)

$$rac{d(A_{Rap})}{dt} = Q_{Rap} imes \left(C_{ArtBld} - \left(rac{C_{Rap}}{P_{Rap}}
ight)
ight)$$

3.4.7 Slowly Perfused Tissues

$$\frac{d(A_{Slw})}{dt} = Perm_{Slw} \times Q_{Slw} \times \left(C_{ArtBld} - \left(\frac{C_{Slw}}{P_{Slw}}\right)\right)$$

3.4.8 Oral Dosing

Equation 3-21

$$\frac{d(A_{OralIn})}{dt} = \frac{PdoseC \times BW \times PulseOral}{OralPulseTime}$$

$$\frac{d(A_{FecOral2})}{dt} = K_{Fec} \times A_{Oral2}$$

$$\frac{d(A_{FecOral2L})}{dt} = K_{Fec} \times A_{Oral2L}$$

Equation 3-24. Amount of D4 in Gut Compartment (mg)

687
$$\frac{d(A_{Oral})}{dt} = pdose - ((K_{Abs} \times A_{Oral} + K_{Abs2} \times A_{Oral}) + (K_{OrTol} \times A_{Oral}))$$

Equation 3-25

$$\frac{d(A_{Oral2})}{dt} = K_{Abs2} \times A_{Oral} - (K_{2Abs} \times A_{Oral2} + RA_{FecOral2})$$

Equation 3-26

$$\frac{d(A_{oralL})}{dt} = (K_{orTol} \times A_{oral}) - (K_{AbsL} \times A_{oralL}) - (K_{Abs2L} \times A_{oralL})$$

Equation 3-27

$$\frac{d(A_{Oral2L})}{dt} = K_{Abs2L} \times A_{OralL} - (K_{2AbsL} \times A_{Oral2L} + K_{Fec} \times A_{Oral2L})$$

Equation 3-28

$$\frac{d(O_{AbsL})}{dt} = K_{AbsL} \times A_{OralL} + K_{2AbsL} \times A_{Oral2L}$$

3.4.9 Dermal Exposure

Equation 3-29. Amount of D4 in Skin at the 1st Application Site (mg)

$$\frac{d(A_{Skin1})}{dt} = RA_{PenSkin1} + \frac{K_{SknDeepOut} \times DermArea_1 \times A_{SknDeep1}}{DermArea_1 + (1 \times 10^{-23})} - \frac{K_{SknDeepOut} \times DermArea_1 \times A_{Skin1}}{DermArea_1 + (1 \times 10^{-23})} - \frac{RA_{DermAbs1} - RA_{Evap1B}}{DermArea_1 + (1 \times 10^{-23})} - \frac{R_{SknDeepOut} \times DermArea_1 \times A_{Skin1}}{DermArea_1 + (1 \times 10^{-23})} - \frac{RA_{DermAbs1} - RA_{Evap1B}}{DermArea_1 + (1 \times 10^{-23})} - \frac{RA_{DermAbs1} - RA_{Evap1B}}{DermAbs1} - \frac{RA_{DermAbs1} - RA_{Evap1B}}{DermAbs1} - \frac{RA_{DermAbs1} - RA_{Evap1B}}{DermAbs1} - \frac{RA_{DermAbs1} - RA_{DermAbs1}}{DermAbs1} - \frac{RA_{DermAbs1}}{DermAbs1} - \frac{RA_{DermA$$

Equation 3-30. Amount of D4 in Skin at the 2nd Application Site (mg)

$$\frac{d(A_{Skin2})}{dt} = RA_{PenSkin2} + \frac{K_{SknDeepOut} \times DermArea_2 \times A_{SknDeep2}}{DermArea_2 + (1 \times 10^{-23})} - \frac{K_{SknDeepOut} \times DermArea_2 \times A_{Skin2}}{DermArea_2 + (1 \times 10^{-23})} - \frac{RA_{DermAbs2} - RA_{Evap2B}}{DermArea_2 + (1 \times 10^{-23})} - \frac{R_{SknDeepOut} \times DermArea_2 \times A_{Skin2}}{DermArea_2 + (1 \times 10^{-23})}$$

3.5 Model Parameters

 Basic physiological parameters used in the model construction are obtained from Brown et al. (1997), which is a common source of physiological values for humans and commonly used laboratory animals. Chemical-specific parameters were obtained by fitting the model predictions to experimental data using a multiple curve-fitting routine. The time-series of the concentrations of D4 and its metabolites in the liver, blood, and urine were used to obtain the MLP parameters (Campbell et al., 2023).

As described by McMullin (2016), the model includes both distributed and diffuse fat compartments.

Distributed fat represents perirenal and abdominal fat. Diffuse fat represents compartments that are more widely distributed throughout the body. Fat tissue parameters were optimized by visual comparisons of the simulated and experimental D4 concentrations in the distributed fat (McMullin et al., 2016).

The data for human exhalation were collected in different exercise or resting states. Those states were represented by changing the alveolar ventilation rate (QP), the cardiac output (QCC), and the blood flow rates to the tissues (Reddy et al., 2008).

McMullin et al. (2016) estimated the human blood:air partition coefficient (PC) by visual optimization of the model PCs to the individual human data from the inhalation study. The tissue:blood PCs for the current human model were calculated using Equation 3-31:

Equation 3-31

$$Tissue: Blood = \frac{Rat\ PC\ tissue: air}{Model\ estimated\ PC\ blood: air}$$

Human and rat Michaelis-Menten (M-M) metabolic parameters for D4 were estimated using experimental data (Table 3-3). McMullin et al. (2016) adjusted the maximal capacity (V_{max}) based on individual data. The affinity constant (K_m) was set to a sufficiently high value to be compatible with linear kinetics. The average value of all human subjects was used for that parameter. Rate constants for the skin absorption were estimated using the dermal study data (Plotzke et al. (2000) as cited in Reddy et al. (2007) and University of Rochester Medical Center (2001)), whereas the other model parameters were taken from the inhalation study (Utell et al., 1998). The rest of the skin-related parameters were obtained by visual optimization of the model to fit the experimental data (McMullin et al., 2016).

Table 3-3. Physiological Parameters for the D4 PBPK Model

Table 3-3. Physiological Parameters for the D4 PBPK Model									
Parameter	Label	F344 (SD) Rat Value	Human Value	Source	Description				
	Physiological Parameters								
Body weight	BW	Study-specific	74	Brown et al. (1997)					
Tissue Volumes	(Fraction of BW)	•							
Blood	VBLDC	0.074	0.079	Brown et al. (1997)					
Diffuse fat	VFATDIFFC	0.063	0.214	Brown et al. (1997) Andersen et al. (2001),					
Distributed fat	VFATDISTC	0.007	0	Brown et al. (1997); Andersen et al. (2001)					
Liver	VLIVC	0.034	0.0257	Brown et al. (1997)					
Lung	VLNGC	0.005	0.0076	Brown et al. (1997)					
Rapidly perfused tissues	VRAPC	0.05	0.0797	Brown et al. (1997)	Assumed to account for 8.4% (10.54% for humans) of body weight along with liver				
Slowly perfused tissues	VSLWC	0.751	0.584	Brown et al. (1997)	Assumed total perfused body weight to be 91%				
Cardiac output	QCC [L/hr/kg ^{0.75}]	15.0	Varies	Brown et al. (1997)					

Parameter	Label	F344 (SD) Rat Value	Human Value	Source	Description
Alveolar ventilation	QPC [L/hr/kg ^{0.75}]	15.0	16.8	Brown et al. (1997)	Assumed equal to QCC when subject is neither asleep nor exercising
Blood Flow (Fra	action of BW)				
Diffuse fat	QFATDIFFC	0.063	0.05	Brown et al. (1997)	Diffuse fat perfusion fraction based on fraction of fat volume represented
Distributed fat	QFATDISTC	0.007	0	Brown et al. (1997)	Diffuse fat perfusion fraction based on fraction of fat volume represented
Liver	QLIVC	0.183	0.227	Brown et al. (1997)	
Rapidly perfused	QRAPC	0.411	0.472	Brown et al. (1997)	Normalized so all blood flow sums to 100%; total output from rapidly perfused compartments assumed to be 69.6%
Slowly perfused	QSLWC	0.336	0.251	Brown et al. (1997)	Normalized so all blood flow sums to 100%; total output from slowly perfused compartments assumed to be 30.1%
		Chemical-Speci	fic Param	eters for D4	
Partition Coeffi	cients (unitless)	Chemical-Speci	iic i aram	ctcl3 for D4	
Blood:air	PBLD	0.85	1.3	Andersen et al. (2001), Campbell et al. (2023)	Optimized to fit single and 15-day inhalation data in F344 rat (Plotzke et al., 2000) and a single inhalation data in human (Utell et al., 1998)
Diffuse fat:air	PFATDIFFAIR	100	100	McMullin et al. (2016)	Optimized to fit single and 15-day inhalation exposure data in F344 rat (Plotzke et al., 2000)
Distributed fat:air	PFATDISTAIR	600	600	McMullin et al. (2016)	Optimized to fit single and 15-day inhalation exposure data in F344 rat (Plotzke et al., 2000)
Liver:air	PLIVAIR	21.2	21.2	McMullin et al. (2016)	Optimized to fit single and 15-day inhalation exposure data in F344 rat (Plotzke et al., 2000)
Lung:air	PLNGAIR	7.9	7.9	McMullin et al. (2016)	Optimized to fit single and 15-day inhalation exposure data in F344 rat (Plotzke et al., 2000)
Rapidly perfused:air	PRAPAIR	8.47	8.47	Andersen et al. (2001) for rat, McMullin et al. (2016) for human	Optimized to fit single and 15-day inhalation exposure data in F344 rat (Plotzke et al., 2000)
Slowly perfused:air	PSLWAIR	8.47	8.47	Andersen et al. (2001) for rat,	Optimized to fit single and 15-day inhalation exposure

Parameter	Label	F344 (SD) Rat Value	Human Value	Source	Description
				McMullin et al. (2016) for human	data in F344 rat (<u>Plotzke et al., 2000</u>)
Diffusion Coeffi	cient (unitless)				
Diffuse fat	PERMFATDIFF	0.17	0.17	Campbell et al. (2017)	Optimized using a single oral exposure data in F344 rat (Domoradzki et al., 2017)
Distributed fat	PERMFATDIST	0.17	0	Campbell et al. (2017)	Optimized using a single oral exposure data in F344 rat (Domoradzki et al., 2017)
Slowly perfused	PERMSLW	1	0.045	McMullin et al. (2016)	Assumed flow limited compartment for rat, a single inhalation exposure in human (Utell et al., 1998)
		Metabo	lic Parame	eters	
Maximal capacity	VMAXC (mg/hr/BW ^{0.75})	3.08 (1.54)	6.08	Andersen et al. (2001)	Optimized to single and 15-day D4 inhalation exposure data in F344 rat (Plotzke et al., 2000) and a single inhalation exposure in human (Utell et al., 1998)
Affinity constant	KM (mg/L)	0.5	0.5	Andersen et al. (2001)	Optimized to fit single and 15-day inhalation exposure data in F344 rat (Plotzke et al., 2000)
Induction of Me	tabolism in Liver	•		1	
Basal level of CYP	CYP0 (AUC/μg protein)	15	15	Sarangapani et al. (2002); (McKim et al., 1998)	Determined from 5-day inhalation exposure in female F344 rats (McKim et al., 1998)
Basal CYP production rate	K0 (AUC/hr/μg protein)	0.483	0.483	Sarangapani et al. (2002)	Computed as CYP0*KELIMCYP
Basal CYP degradation rate	KELIMCYP (/hr)	0.0322	0.0322	Sarangapani et al. (2002)	Optimized using a 5-day inhalation data in female F344 rat (McKim et al., 1998)
Maximum CYP production rate	KMAX (AUC/hr/μg protein)	4 (2)	4	Campbell et al. (2023)	Optimized to fit 5-day F344 rat inhalation, (McKim et al., 1998) and 15-day SD rat inhalation data (Schmitt et al., 2023)
Dissociation constant CYP induction	KDLIV (μM)	0.67	0.67	Sarangapani et al. (2002)	Initial values obtained by visually fitting to 5-day inhalation exposure date in female Fischer 344 rat (McKim et al., 1998). These values used as seed values for the Nedler-Mead optimization algorithm

September 2025							
Parameter	Label	F344 (SD) Rat Value	Human Value	Source	Description		
Fraction of mass returning from 1st deep liver compartment available for metabolism	FRLIDM	0.002	0.002	Campbell et al. (2017)	Optimized to bolus data in male F344 rat (<u>Domoradzki</u> et al., 2017)		
	Mobile Lipid 1	Pool (MLP) Para	meters (L/	hr, scaled to tissue volu	ume)		
Production rate of MLP in liver	KMLP	0.00062	0.057	Adjusted in Campbell et al. (2023)	Optimized to fit 28-day inhalation data in male F344 rat (Meeks et al., 2022) with minimization of sum of squared errors. Parallelogram approach was utilized for human		
Production rate of MLP in deep liver	KMLPDEEP	0.0000525	0.0049	Campbell et al. (2023)	Optimized to fit 28-day inhalation data in male F344 rat (Meeks et al., 2022) with minimization of sum of squared errors. Parallelogram approach was utilized for human		
Production of MLP in fat (distributed and diffuse)	KMLPF	0.000780	0.072	Adjusted in Campbell et al. (2023)	Optimized to fit 28-day inhalation data in male F344 rat (Meeks et al., 2022) with minimization of sum of squared errors. Parallelogram approach was utilized for human		
Clearance from MLP compartment to liver	KREMOVALLMLP	0.0196	0.14	Adjusted in Campbell et al. (2023)	Optimized to fit 28-day inhalation data in male F344 rat (Meeks et al., 2022) with minimization of sum of squared errors. Parallelogram approach was utilized for human		
Clearance from MLP compartment to fat (distributed and diffuse)	KREMOVALFMLP	0.00316	0.022	Adjusted in Campbell et al. (2023)	Optimized to fit 28-day inhalation data in male F344 rat (Meeks et al., 2022) with minimization of sum of squared errors; parallelogram approach was utilized for human		
		_		ents (L/hr, scaled to tis			
Into 1st deep lung compartment	KLNGDEEP1IN	0.018	0.018	McMullin et al. (2016)	Optimized to fit single and 15-day D4 inhalation exposure data in F344 rat (Plotzke et al., 2000) using log of likelihood function		
Out of 1st deep lung compartment	KLNGDEEP1OUT	0.0166	0.0166	McMullin et al. (2016)	Optimized to fit single and 15-day D4 inhalation exposure data in F344 rat (Plotzke et al., 2000) using log of likelihood function		

	September 2025						
Parameter	Label	F344 (SD) Rat Value	Human Value	Source	Description		
Into 1st deep liver compartment	KLIVDEEPIIN	0.5	0.5	Campbell et al. (2017)	Optimized using single oral exposure data in F344 rat (Domoradzki et al., 2017)		
Out of 1st deep liver compartment	KLIVDEEP1OUT	0.1	0.1	Campbell et al. (2017)	Optimized using single oral exposure data in F344 rat (Domoradzki et al., 2017)		
Into 2nd deep liver compartment	KLIVDEEP2IN	0.0012	0.0012	Campbell et al. (2017)	Optimized using single oral exposure data in F344 rat (Domoradzki et al., 2017)		
Out of 2nd deep liver compartment	KLIVDEEP2OUT	0.007	0.007	Campbell et al. (2017)	Optimized using single oral exposure data in F344 rat (Domoradzki et al., 2017)		
Oral Absorption	n Rate Constants (hr ⁻¹)					
Absorption rate 1st compartment	KABS	0.034	0.034	Campbell et al. (2017)	Optimized using single oral exposure data in F344 rat (Domoradzki et al., 2017)		
Transfer 1st to 2nd compartment	KABS2	0.1	0.1	Campbell et al. (2017)	Optimized using single oral exposure data in F344 rat (Domoradzki et al., 2017)		
Absorption rate 2nd compartment	K2ABS	0.17	0.17	Campbell et al. (2017)	Optimized using single oral exposure data in F344 rat (Domoradzki et al., 2017)		
Transfer from free to lipoprotein- associated absorption	KORTOL	0.17	0.35	Campbell et al. (2017)	Optimized using single oral exposure data in F344 rat (Domoradzki et al., 2017)		
Absorption rate 1st lipoprotein- associated compartment	KABSL	0.2	0.55	Campbell et al. (2017)	Optimized using single oral exposure data in F344 rat (Domoradzki et al., 2017)		
Transfer 1st to 2nd lipoprotein- associated compartment	KABS2L	0.134	0.134	Campbell et al. (2017)	Optimized using single oral exposure data in F344 rat (Domoradzki et al., 2017)		
Absorption rate 2nd lipoprotein- associated compartment	K2ABSL	0.067	0.08	Campbell et al. (2017); Campbell et al. (2023)	Optimized using single oral exposure data in F344 rat (Domoradzki et al., 2017)		
Fecal excretion of unabsorbed oral dose	KFEC	0.15	0.15	Campbell et al. (2017)	Optimized using single oral exposure data in F344 rat (Domoradzki et al., 2017)		
Delay in fecal elimination for transit	FECDELAYP	7	0	McMullin et al. (2016)	Estimated gastrointestinal transit in rat		

	I	*	111001 202	1	
Parameter	Label	F344 (SD) Rat Value	Human Value	Source	Description
Uptake into Tiss	sue from Lipoprotein-A	Associated Absor	ption (L/h	r, scaled to tissue volu	me)
Into deep blood compartment from oral absorption lipid	KREMOVALF	0.5	0.5	Campbell et al. (2017)	Optimized using single oral exposure data in F344 rat (Domoradzki et al., 2017)
Into distributed fat compartment from oral absorption lipid	KREMOVALFDIST	0.5	0.5	Campbell et al. (2017)	Optimized using single oral exposure data in F344 rat (Domoradzki et al., 2017)
Into liver compartment from oral absorption lipid	KREMOVALL	25	25	<u>Campbell et al.</u> (2017)	Optimized using single oral exposure data in F344 rat (Domoradzki et al., 2017)
Fraction of liver compartment removal to 1st deep liver compartment	FRACOLDEEP1	0.4	0.4	Campbell et al. (2017)	Optimized using single oral exposure data in F344 rat (Domoradzki et al., 2017)
Fraction of liver compartment removal to 2nd deep liver compartment	FRACOLDEEP2	0.0005	0.0005	Campbell et al. (2017)	Optimized using single oral exposure data in F344 rat (Domoradzki et al., 2017)
		Dermal Abso	orption Pa	rameters	
Evaporation rate from skin surface (mg/hr-cm²)	KEVAPC	0	9	McMullin et al. (2016)	Measured in vitro in McMullin et al. (2016)
Absorption into blood from skin (cm/hr)	KSKNBLD	0	0.045	McMullin et al. (2016)	Visually optimized to fit a single dermal exposure in human ((Plotzke et al., 2000) as cited in (Reddy et al., 2007))
Out of deep skin compartment (hr ⁻¹)	KSKNINC	0		McMullin et al. (2016)	Visually optimized to fit a single dermal exposure in human ((Plotzke et al., 2000)) as cited in (Reddy et al., 2007))
Rate evaporated from skin tissue (cm/hr)	KSKNOUTC	0	380	McMullin et al. (2016)	Visually optimized to fit single dermal exposure data in humans ((Plotzke et al., 2000) as cited in (Reddy et al., 2007))
Into deep skin compartment (hr ⁻¹)	KSKNDEEPIN	0	1	McMullin et al. (2016)	Visually optimized to fit a single dermal exposure in human (Plotzke et al. (2000) as cited in Reddy et al. (2007))
Out of deep skin compartment (hr ⁻¹)	KSKNDEEPOUT	0	0.1	McMullin et al. (2016)	Visually optimized to fit a single dermal exposure in human (Plotzke et al. (2000) as cited in Reddy et al. (2007))

750 751

Table 3-4. List of State Variables, Non-Constant, and Other Model Parameters

Parameters	Description			
AARTBLD	Amount of D4 in arterial blood "free" (mg)			
AARTBLDDLP	Amount of D4 in dietary blood lipid in arterial blood (mg)			
AARTBLDMLP	Amount of D4 in blood lipid in arterial blood (mg)			
ACYP	Amount of induction of metabolism in liver by D4 (mg)			
ADERMABS1	Amount of D4 in the blood from dermal absorption at the first application site (mg)			
ADERMABS2	Amount of D4 in the blood from dermal absorption at the second application site (mg)			
ALIVDEEP1	Amount of D4 in 1st deep liver compartment (mg)			
AEVAP1B	Amount of D4 evaporated from the first application site (mg)			
AEVAP2B	Amount of D4 evaporated from the second application site (mg)			
ALIVDEEP2	Amount of D4 in 2nd deep liver compartment (mg)			
AMET	Amount of D4 metabolized in liver (mg)			
AARTBLDTOT	Total amount of D4 in arterial blood (mg)			
AORAL	Amount in gut compartment from oral dosing (mg)			
AORAL2	Amount in second gut compartment from oral dosing (mg).			
AORALIN	Amount of oral intake (mg)			
AORAL2L	Lipid-associated uptake of D4, second compartment (mg)			
AORALL	Lipid-associated oral uptake amount of D4 (mg)			
APENSKIN1	Amount of D4 entering skin at the first application site (mg)			
APENSKIN2	Amount of D4 entering skin at the second application site (mg)			
ARAP	Amount of D4 in rapidly perfused tissues (mg)			
ASKIN1	Amount of D4 in skin at the first application site (mg)			
ASKIN2	Amount of D4 in skin at the second application site (mg)			
ASKNDEEP1	Amount of D4 in deep skin compartment at the first application site (mg)			
ASKNDEEP2	Amount of D4 in deep skin compartment at the second application site (mg)			
ASLW	Amount of D4 in slowly perfused tissues (mg)			
AVENBLDDLP	Amount of D4 in dietary blood lipid in venous blood (mg)			
AVENBLDMLP	Amount of D4 in blood lipid in venous blood (mg)			
CARTBLD	Arterial blood concentration (mg/L)			
CARTBLDDLP	Concentration of D4 in dietary blood lipid in arterial blood (mg)			
CARTBLDTOT	Total concentration of D4 in arterial blood (mg/L)			
CFATDIFF	Diffuse fat concentration (mg/L)			
CRAP	Concentration of D4 in rapidly perfused tissues (mg/L)			
CSLW	Concentration of D4 in slowly perfused tissues (mg/L)			
CVFATDIFF	$((1.0 - PERMFATDIFF) \times CARTBLD) + (PERMFATDIFF \times (CFATDIFF / PFATDIFF))$			
CVLIV	(CLIV / PLIV) wherein CLIV is concentration in the liver and PLIV is liver:blood partition coefficient			

Parameters	Description			
CVLIVDEEP1	Mass from 1st deep liver compartment available for metabolism; equals ALIVDEEP1*FRLIDM/VLIV wherein FRLIDM is the fraction of mass returning from 1st deep liver compartment available for metabolism			
CVLNG	Lung concentration (mg/L)			
CYP0	Basal level of CYP (AUC/µg protein)			
DERMAREA1	Dermal exposure surface area 1st location (cm2)			
DERMAREA2	Dermal exposure surface area 2d location (cm2)			
FACTOR	ACYP/CYP0			
KREMOVALF	Uptake into deep blood compartment from oral absorption lipid tissue from lipoprotein-associated absorption (L/hr; scaled to tissue volume)			
KREMOVALFDIST	Uptake into distributed fat compartment from oral absorption lipid tissue from lipoprotein-associated absorption (L/hr; scaled to tissue volume)			
KREMOVALL	Uptake into liver compartment from oral absorption lipid tissue from lipoprotein-associated absorption (L/hr; scaled to tissue volume)			
OABS	Oral absorption amount (mg)			
ORALPULSETIME	Length of administration of oral dose (hr)			
PDOSEC	Oral dose (mg/kg)			
PFATDIFF	Diffuse fat:blood partition coefficient; PFATDIFFAIR / PBLD			
PFATDIST	Distributed fat:blood partition coefficient; PFATDISTAIR / PBLD			
PRAP	Rapidly perfused:blood partition coefficient for D4; PRAPAIR / PBLD			
PSLW	Slowly perfused:blood partition coefficient for D4; PSLWAIR / PBLD			
Pulseoral	A parameter takes the pulsatile administration of oral dose into account			
QC	Cardiac blood flow. QC maintains flow balance during human exercise simulation (L/hr/kg ^{0.75}) QC = QLIV + QFATDIFF + QFATDIST + QRAP + QSLW			
QRAP	Cardiac output (blood flow) to rapidly perfused tissues (L/hr)			
QSLW	Cardiac output to slowly perfused tissues (L/hr)			
RAFECAORAL2L	Fecal excretion rate of the lipid-associated oral uptake, second compartment (mg/hr)			
RAFECORAL2	Fecal excretion rate of the oral uptake, second compartment (mg/hr)			
RALEAVEDLPF	Rate of D4 in dietary blood lipid leaving arterial blood to fat (mg/hr)			
RALEAVEDLPL	Rate of D4 in dietary blood lipid leaving arterial blood to liver (mg/hr)			
RALIVDEEP1	Amount of D4 in 1st deep liver compartment (mg)			
RALEAVEDLPFDIST	Rate of D4 in dietary blood lipid leaving arterial blood to distributed fat (mg/hr)			
RALEAVEMLPF	Rate of D4 in mixed lipid leaving arterial blood to fat (mg/hr)			
RALEAVEMLPL	Rate of D4 in mixed lipid leaving arterial blood to the liver (mg/hr)			
RAPRODMLPL	Rate of D4 in blood lipid produced in liver (mg/hr). Equals KMLP*CVLIV*VLIV wherein KMLP is the production rate of MLP in liver (L/hr; scaled to tissue volume)			
RAPRODMLPFDIFF	Rate of D4 in blood lipid produced in diffuse fat (mg/hr); equals KMLPF*CVFATDIFF*VFATDIFF			
RAPRODMLPFDIST	Rate of D4 in blood lipid produced in distributed fat (mg/hr); KMLPF*CVFATDIST*VFATDIST			
RAPRODMLPLDEEP	Rate of D4 in blood lipid produced in deep liver (mg/hr). Equals KMLPDEEP*VLIV*(ALIVDEEP1/VLIV) wherein KMLPDEEP is the production rate of MLP in deep liver			

Parameters	Description		
RAMET2	The mass of deep 1 liver available for metabolism		
ROABS	Rate of oral absorption (mg/hr)		
ROABSL	Lipid-associated uptake of D4 (oral dose)		
VARTBLD	Arterial blood volume		
VMAX	$VMAXC \times BW^{0.75}$		
VVENBLD	Venous blood volume		

3.6 Model Simulations

The current model covers oral and inhalation routes of exposure in rats. The empirical oral exposure data come from experiments in which adult male and female CDF (Fischer344)/CrlBr rats were administered 30 mg/kg of radiolabeled D4 (<u>Domoradzki et al., 2017</u>).

For inhalation modeling, empirical data were collected from single- and multiple-exposure experiments in which groups of male and female F344 rats were administered from 7 to 700 ppm of D4 (<u>Campbell et al., 2017</u>; <u>Plotzke et al., 2000</u>). In single-exposure studies, these animals were exposed to ¹⁴C-D4 vapor for 6 hours in a chamber. In the multiple-exposure case, animals were exposed to unlabeled D4 for 14 days, followed by a single exposure to ¹⁴C-D4 vapor the day after. In another inhalation study, SD and F344 rats were exposed to 700 ppm D4 vapor for 1, 15, and 28 days. Concentrations of D4 in the plasma and fat were measured during and after exposure (<u>Meeks et al., 2022</u>).

In human inhalation studies, male subjects were exposed to 10 ppm of ¹⁴C-D4 during intermittent exercises (<u>Utell et al., 1998</u>). The amount of D4 in blood, exhaled breath, and urine was measured during and 1, 3, and 7 days after exposure, respectively.

In human dermal experiments, ¹³C-D4 was applied to the axillae of male (1.4 g) and female (1.0 g) volunteers (Plotzke et al. (2000) as cited in University of Rochester Medical Center (2001) and Reddy et al. (2007)). After five minutes, D4 in the blood and exhaled breath was measured.

3.7 Software

The original version of the model (McMullin et al., 2016) was written in acslX version 11.8.4 (AEgis Technologies Group, Inc., Huntsville, Alabama, USA). It was translated into MCSim (version 6.0.1) (Bois, 2009), which was then translated into C+. RTools (version 3.5.0.4) was then used to compile the C+ file and allow for integration with the deSolve package (Soetaert et al., 2010). R (version 3.5.3) and RStudio (version 1.0.136) were used to edit model files and run simulations (Campbell et al., 2023).

4.1 Model Evaluation

Inhalation Predictions for F344 Rats

Figure 4-1 shows the model prediction results for a time-series of D4 in plasma and fat of F344 rats during and after inhalation exposure to 700 ppm of D4 for 28 consecutive days. Closed circles show experimental data from Meeks et al. (2022). Compared with previous models, the current one offers significantly improved accuracy in the prediction of D4 concentrations in plasma and fat, specifically for postexposure times (Campbell et al., 2023).

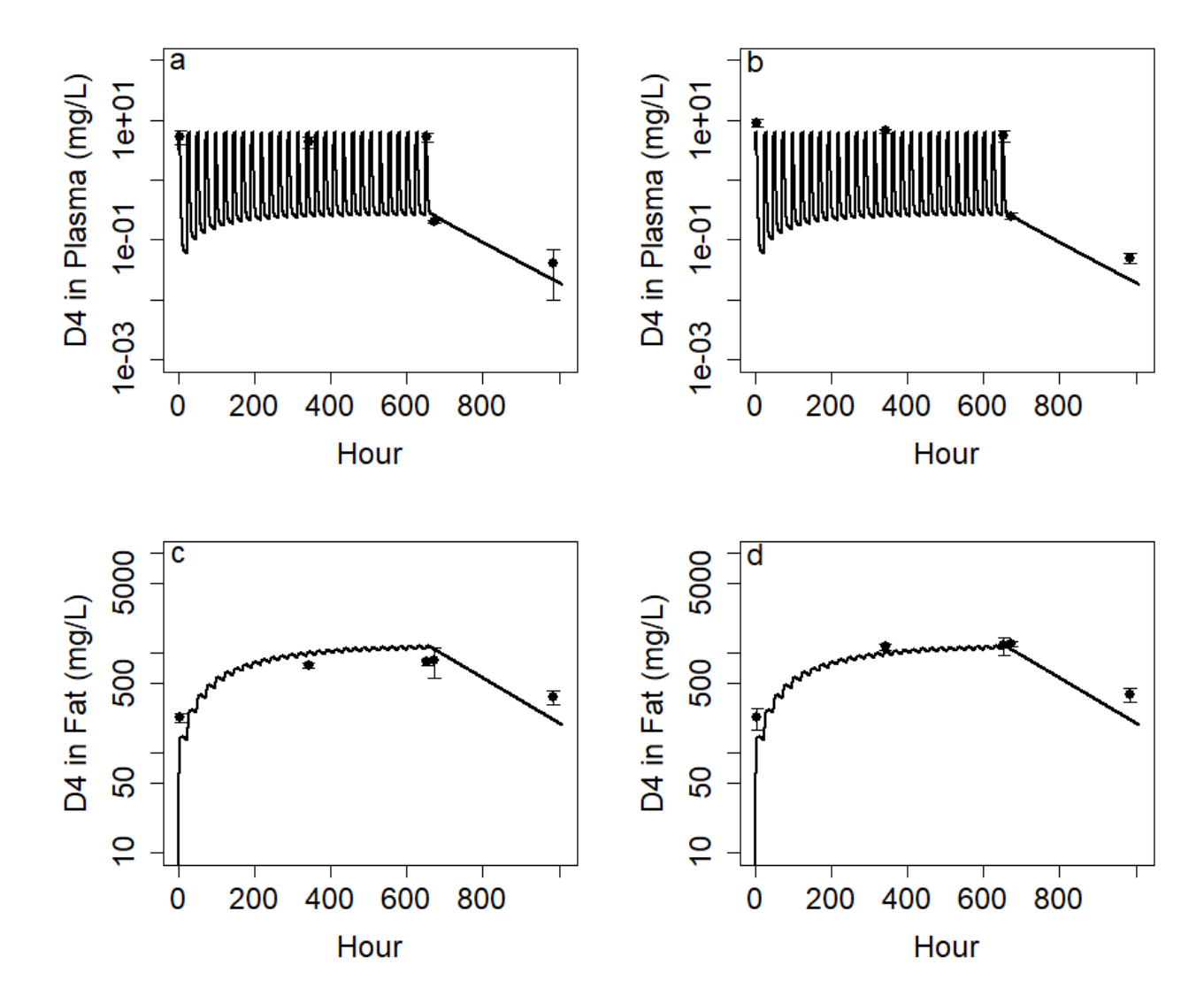


Figure 4-1. Comparison of Model Simulations and F344 Rat Inhalation Experimental Data Experimental data (Meeks et al., 2022) for F344 rats (closed circles) and time-series from the Campbell et al. (2023) model simulation (lines) for the concentration of D4 in plasma of males (a) and females (b) and fat for males (c)

and females (d). Rats were exposed via inhalation to 700 ppm of D4 (Meeks et al., 2022). The plots are regenerated using the model codes from Campbell et al. (2023).

Campbell et al. (2023) reported a 15-fold reduction in sum of squared error in prediction of D4 concentration in the blood of F344 rats. **Error! Reference source not found.** Table 4-1 shows the sum of squared errors (sum of log model – log data squared) when simulating male and female F344 rats exposed for 28 days to 700 ppm D4 (6 hr/day, 7 days/week) (Meeks et al., 2022). The data are generated from the model codes to reproduce Table 3 in Campbell et al. (2023).

Table 4-1. Sum of Squared Errors for the Campbell 2017 and 2023 Models Compared with Inhalation Data in F344 Rats

Sex	Tissue	Sum of Squared Errors (Sum of Log Model Minus Log Data Squared)		
		2017 Model	2023 Model	
Male	Blood	10.96	0.68	
	Fat	3.57	0.80	
	Total Error	14.53	1.48	
Female	Blood	11.62	0.86	
	Fat	3.34	0.58	
	Total Error	14.96	1.44	

Oral Predictions for F344 Rats

The model code from Campbell et al. (2023) was then used to simulate male F344 rat oral exposure data from Domoradzki et al. (2017), as seen in Figure 4-2. The results are comparable to Figure 7 in Campbell et al. (2017), although the 2023 model predicts the sum of the plasma concentration of D4 and its metabolites more reasonably.

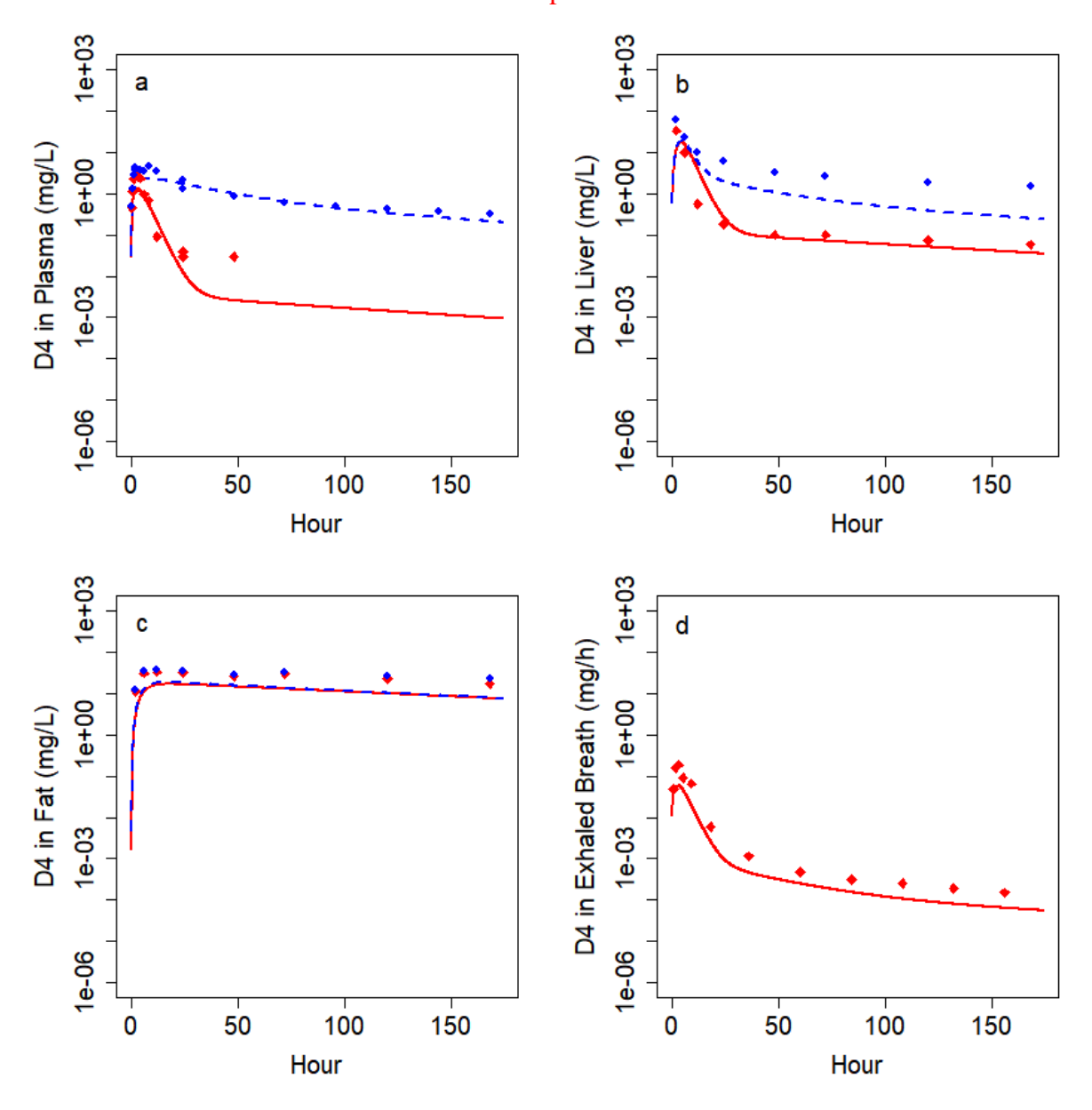


Figure 4-2. Comparison of Model Simulations and Male F344 Rat Oral Experimental Data Experimental data (Domoradzki et al., 2017) (closed shapes) and time-series from the 2023 Campbell model simulation (lines) for the concentration of D4 in (a) plasma, (b) liver, and (c) fat in male F344 rats after oral administration of 30 mg/kg. The rate of D4 generated in exhaled breath is shown in (d). Red lines and closed diamonds represent the parent D4 and blue diamonds and blue dashed lines represent the total concentration of D4 and its metabolites. The plots are generated using the model codes from 2023 Campbell model but are not published in Campbell et al. (2023).

Inhalation and Dermal Predictions for Humans

The model also predicts D4 exhaled breath and plasma concentrations for inhalation and dermal exposure routes in humans as seen in Figure 4-3. Modeled results were compared with human dermal data from Plotzke et al. (2000) (as cited in University of Rochester Medical Center (2001) and Reddy et al. (2007)) in which 1.4 g ¹³C-D4 was applied to skin axilla of male subjects. The modeled concentrations are slightly overestimated for the dermal exposure. To further evaluate the model's capability in simulating experimental data, exposure parameters in the human dermal study by Biesterbos et al. (2015) were used as inputs to the PBPK model and compared with the data from

Plotzke et al. (2000) (as cited in University of Rochester Medical Center (2001) and Reddy et al. (2007)). Simulation results are presented in Figure 4-4. In the Biesterbos experiments, 8.6 g of D4 were applied to the forearm of adult subjects every 10 minutes for 1 hour. D4 concentration was measured during and up to 6 hours after exposure. Unlike in the study by Plotzke et al. (2000) (as cited in Reddy et al. (2007)), the post-exposure concentrations in Biesterbos et al. (2015) did not exceed background levels and the model substantially underpredicted experimentally derived values.

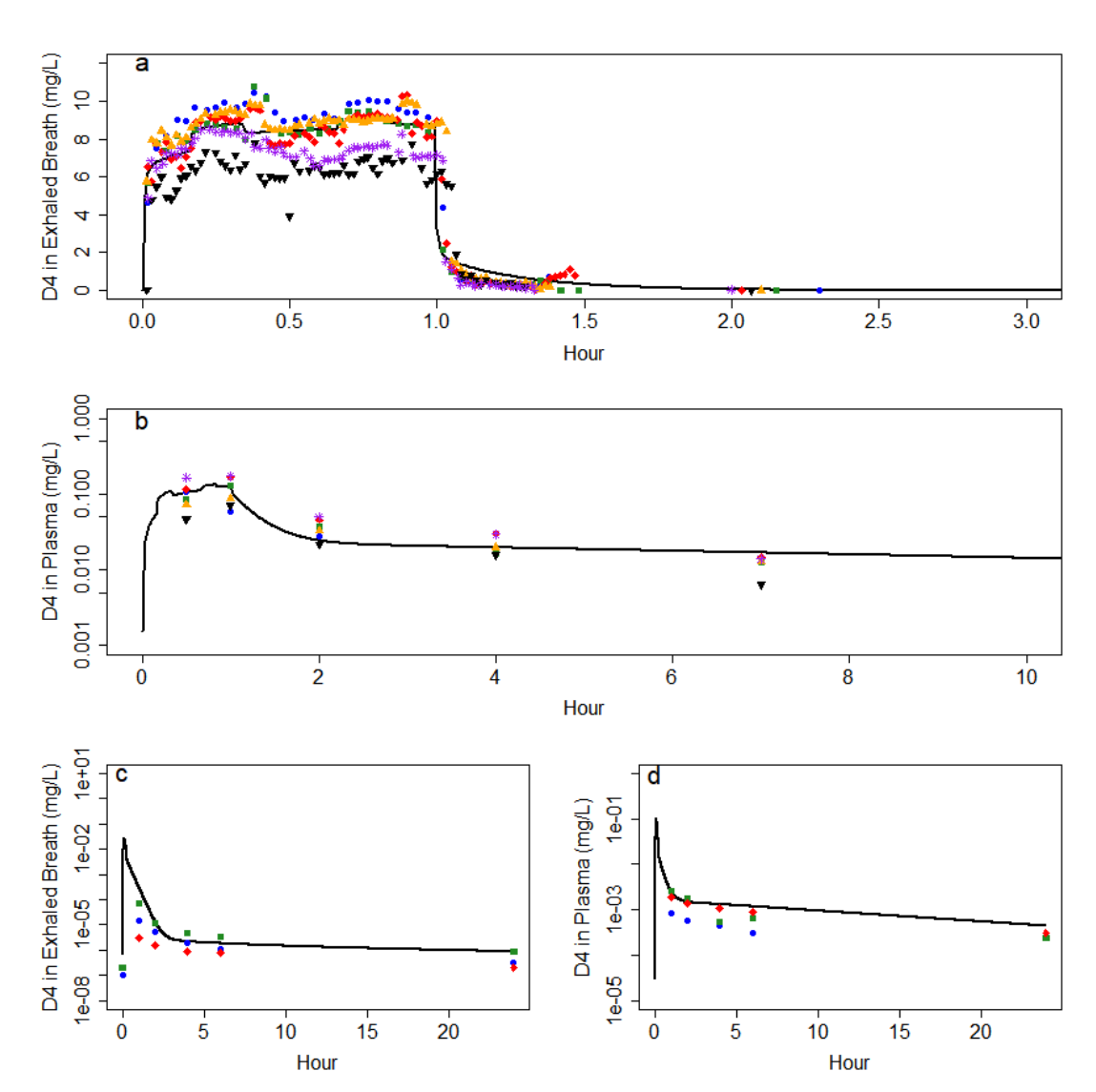


Figure 4-3. Comparison of Model Simulations and Human Inhalation and Dermal Data Experimental data (closed shapes) and the 2023 Campbell model simulations (lines) of D4 in (a) exhaled breath and (b) plasma of human subjects during and after 10 ppm D4 vapor exposure (<u>Utell et al., 1998</u>) or (c) exhaled breath and (d) plasma during and after a single application of 1.4 g 13C-D4 to skin axilla of male subjects ((<u>Plotzke et al., 2000</u>) as cited in (<u>Reddy et al., 2007</u>)). Different shapes represent different individuals. The plots are generated from the model codes to reproduce Figure 7 in Campbell et al. (2023).

Dermal Predictions for Humans Using Two Datasets

To further evaluate the model's capability in simulating experimental data, exposure parameters in another human dermal study (<u>Biesterbos et al., 2015</u>) were used as inputs to the PBPK model. In those experiments, 8.6 g of D4 were applied to the forearm of adult subjects every 10 minutes for 1 hour. D4

concentration was measured during and up to 6 hours after exposure. Biesterbos et al. (2015) concluded that the D4 concentration in exhaled breath was not significantly higher than the background air concentration. Figure 4-4 presents simulation results for Biesterbos et al. (2015) as well as for Plotzke et al. (2000) (as cited in Reddy et al. (2007)), which is the human dermal dataset already used to build parameters for the 2023 Campbell model.

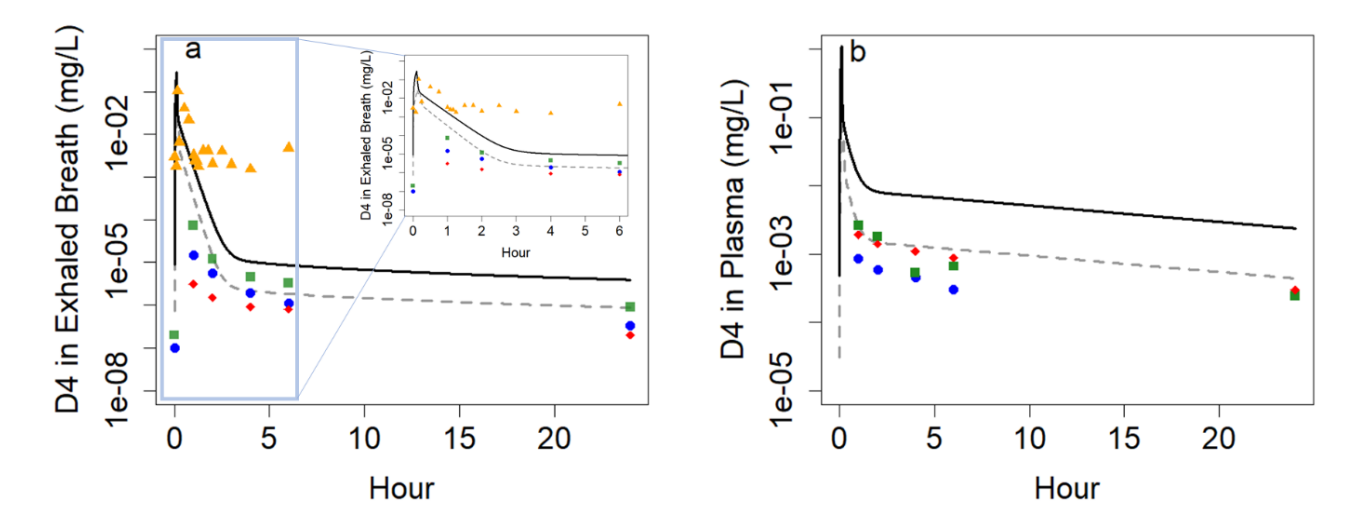


Figure 4-4. Comparison of Model Simulations with Human Dermal Data from Two Datasets Experimental data (closed shapes) and the 2023 Campbell model simulations (lines) of D4 in (a) exhaled breath and (b) plasma of humans. Black solid lines show simulation of <u>Biesterbos et al. (2015)</u> and gray dashed lines show simulation of (<u>Plotzke et al. (2000)</u> as cited in <u>Reddy et al. (2007)</u>). Closed squares, circles, and diamonds represent exhaled breath data for individual subjects in (<u>Plotzke et al., 2000</u>) (as cited in (<u>Reddy et al., 2007</u>)). Closed triangles represent mean (n = 6) D4 concentrations measured in <u>Biesterbos et al. (2015)</u>, digitized with WebPlot Digitizer (https://automeris.io/wpd/). D4 is not measured in plasma in <u>Biesterbos et al. (2015)</u>.

Oral Predictions for Humans

Existing literature suggests that there is no time course data for oral exposure in humans except for a two-week study (<u>Dow Corning</u>, <u>1998a</u>) in which subjects were administered 12 mg of D4 per day via 1 mL of corn oil. The control group was given a placebo. D4 concentrations in plasma were measured for baseline and after the first and second weeks of exposure. Averages and standard deviations of the experimental data are represented in **Error! Reference source not found.**. The PBPK model predicts D4 concentration in plasma to be 0.011 and 0.012 mg/L (approximately 11 and 12 ng/g) for the first and second week, respectively. The predicted values are close to those in the experiment as seen in Figure 4-6.

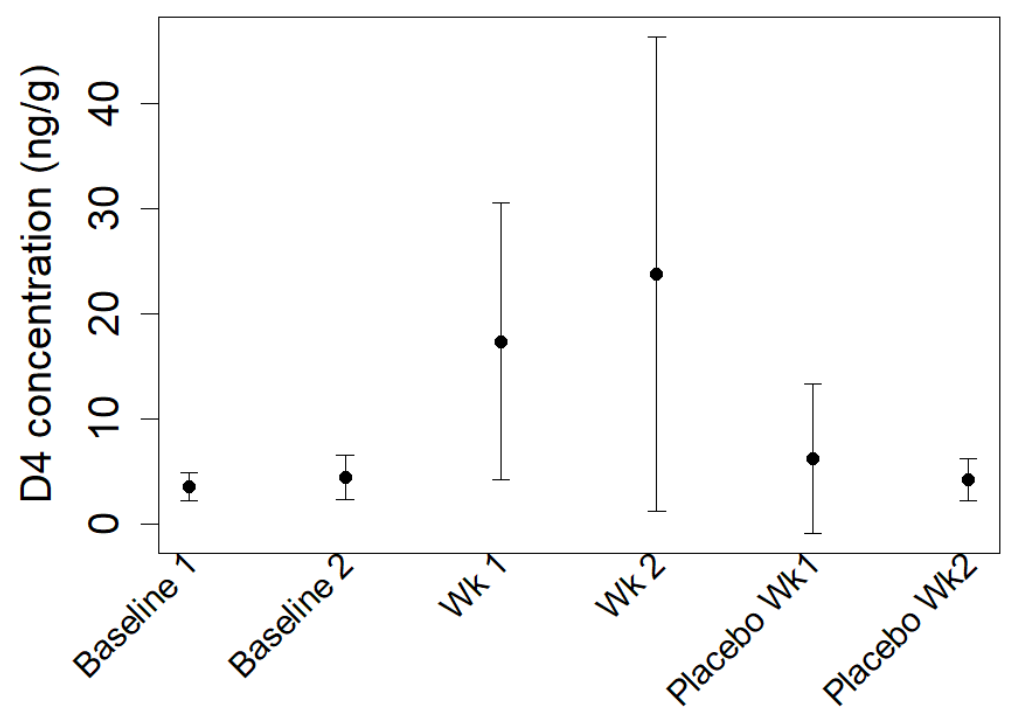


Figure 4-5. D4 Concentrations in Plasma from Human Oral Experimental Data

Dow Corning (1998a) collected data from 12 healthy subjects. Baseline D4 measurements were taken at the beginning of the study. Subjects were then administered 12 mg of D4 per day in 1 mL of corn oil for two weeks or were given a placebo for 2 weeks. Weekly averages and standard deviations were computed.

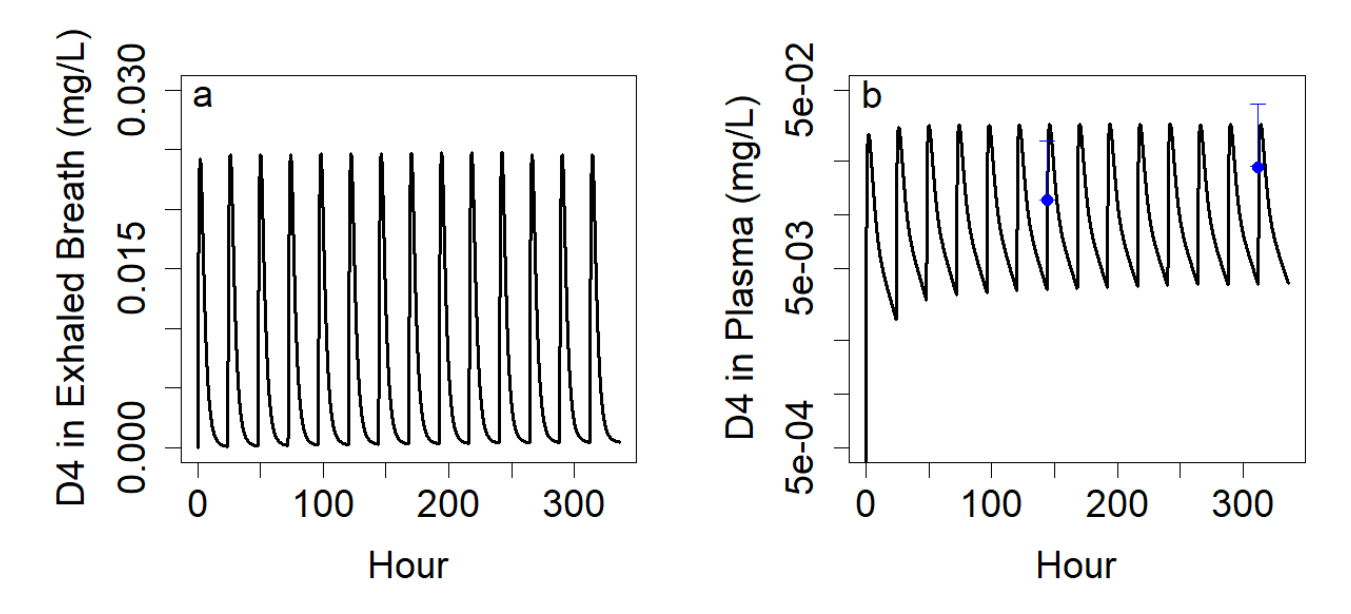


Figure 4-6. Simulation of Repeated-Dose Oral Exposure in HumansThe 2023 Campbell model was run with an exposure scenario from <u>Dow Corning (1998a)</u> to simulate the repeated-dose oral exposure in humans (lines) in (a) exhaled breath and (b) plasma of the subjects. Closed circles show weekly average concentrations offset by placebo concentrations from the experimental data presented in <u>Dow Corning (1998a)</u>.

4.2 Sensitivity, Uncertainty, and Variability Analyses

Local sensitivity analysis was performed for the input parameters for both species and different routes of exposure. Equation 4-1 was used for local sensitivity analysis.

Equation 4-1

884

885 886

887

888 889

890

891 892

893

894

895 896

897 898

899

900 901

902

903

Normalized sensitivity coefficient =
$$\frac{\% \text{ output change}}{\% \text{ parameter change}}$$

The model was first run using the default parameters. Then, the model was run by increasing the default value of only one parameter at a time by 1 percent. An increase of 1 percent was chosen to be consistent with sensitivity in Campbell et al. (2023). The results of each of these runs were compared against the original run. The outputs of interest were concentration in compartments for times at the end of exposure and the last time point of the postexposure period.

Table 4-2 through Table 4-6 show the input parameters that result in a normalized sensitivity coefficient of 0.2 or greater for different exposures in rats and humans.

Table 4-2. D4 PBPK Model Input Parameters That Result in a Normalized Sensitivity Coefficient of 0.2 or Greater in Listed Compartments (Blood, Liver, Fat, and Lung) of F344 Rat at the End of 28-day Inhalation Exposure and the End of 14-day Postexposure Period

Parameter (units)	Label	Sex	E	nd of H	Exposu	re		2 Week nd of E		
A SS: ait as a supple of the same (many III)	VM.	F		O P	33	*			31	*
Affinity constant (mg/L)	KM	M		@P	3:3	*			95	*
A1 1 (I /I . /I . / 75)	ODC	F			33	*			33	_
Alveolar ventilation (L/hr/kg0.75)	QPC	M			33	*			33	_
D 1 CVD 1 1 (1 -1)	WELD COVE	F		@	33	*	۵		33	*
Basal CYP degradation rate (hr ⁻¹)	KELIMCYP	M		@	33	*	۵		33	*
Basal CYP production rate	IZO.	F			35	*		_	33	M
(AUC/hr/μg protein)	K0	M			33	*	۵		33	*
Blood flow in diffuse fat (fraction of	OF A TIDIFEC	F		O P	33	*	۵		33	*
BW)	QFATDIFFC	M		O P	33	*	۵		33	(
Blood flow in distributed fat	OF A TRUCTO	F	_	@P	33	*	۵		33	*
(fraction of BW)	QFATDISTC	M	_	O P	33	*			35	(
Disciplination of DW	OL IV.C	F		@	33	_	۵		33	*
Blood flow in liver (fraction of BW)	QLIVC	M		@	33	*	۵		33	*
Blood flow in rapidly perfused	on and	F			33	*		_	35	*
tissues (fraction of BW)	QRAPC	M			35	*			33	*
Blood flow in slowly perfused	OGI WG	F			98	*		_	33	*
tissues (fraction of BW)	QSLWC	M			98	*			33	*
Blood volume (fraction of BW)	VBLDC	F		_	_	_	۵	_	_	_

Parameter (units)	Label	Sex	E	nd of I	Exposu	re		2 Week and of E		
		M		_	_	*	•	_	_	_
Blood:air partition coefficient	DDI D	F	۵		33	*	۵		31	*
(unitless)	M	•		33	*	۵		3 :	*	
D 1 21/4)	DW	F			35	*			33	*
Body weight (kg)	BW	M			33	*			33	*
	000	F			33	*			31	*
Cardiac output (L/hr/kg0.75)	QCC	M			33	*			31	*
Clearance from MLP compartment to fat (distributed and diffuse) (L/hr;	KREMOVALFMLP	F		_	_	*	۵	_	_	_
scaled to tissue volume)		M		_	_	*		_	_	_
Clearance from MLP compartment to liver (L/hr; scaled to tissue	KDEMOVALIMI D	F		_	_	*	۵	_	_	_
volume)	KKEWO V ALLWEI	M		_	_	*		_	_	_
Diffuse fat diffusion coefficient	DEDMEATDIEE	F			_	_			31	*
(fraction of tissue blood flow)	PERMITATUIFF	M			_	*		O P	_	
Diffuse for volume (freetien of DW)	VEATDIEEC	F			95	_			33	
Diffuse fat volume (fraction of BW)	VFAIDIFFC	M			33	*			33	*
Diffuse fat:air partition coefficient (unitless)	DE A TIDICE A ID	F	-	-	_	_		_	_	*
	FFAIDIFFAIR	M	ı	_	_	*	_	_	_	_
Dissociation constant CYP	KDLIV	F			8 3	*			31	*
induction (µM)	KDLIV	M			8 5	*			35	*
Distributed fat diffusion coefficients	DEDMEATDIST	F	_	_	33	*			31	*
(fraction of tissue blood flow)	FERWITAT DIST	M	_	_	33	*			31	*
Distributed fat volume (fraction of	VEATDISTC	F	_	_	33	M			31	*
BW)	VFAIDISTC	M	_	_	95	(1)			31	*
Distributed fat:air partition	DEATDISTAID	F	_	_	35	(1)		_	31	*
coefficient (unitless)	FFATDISTAIR	M	_	_	35	M			31	*
Fecal excretion of metabolite (1 and	KEECSCI SC	F	_	_	_	M	_	_	_	_
2) (BW-0.25/hr)	MECSCLSC	M	_	_	_	*	_	_	_	_
Fraction of mass returning from 1st		F	_		_	(1)			_	_
deep liver compartment available for metabolism (unitless)	FRLIDM	M	-		_	h	٥	(P)	_	-
Induction of metabolism in liver,	CYP0	F			35	*			33	*
basal level of CYP (AUC/μg protein)	CIPU	M			33	*			35	*
Inhalation concentration (ppm)	CONC	F	_	_	_	_	_	_	_	_
imaiation concentration (ppin)	COINC	M	•		35	*	•		31	^
Liver volume (fraction of BW)	VLIVC	F			_	_	•	O P	33	*
Error volume (maction of DW)	, LI V C	M			_	(1)			93	*

Parameter (units)	Label	Sex	E	nd of I	Exposu	re		2 Week		
Liver:air partition coefficient		F			_	(1)	_		_	_
(unitless)	PLIVAIR	M			3:3	*	۵		_	_
		F	_	_	_	_		_	33	_
Lung volume (fraction of BW)	VLNGC	M	_	_	_	_	_	_	_	_
Lung:air partition coefficient	PLNGAIR	F	ı	_	_	^	_	_	_	^
(unitless)	FLNOAIK	M	-	_	_	*	_	_	_	*
Mass transfer into 1st deep lung compartment (L/hr; scaled to tissue	KLNGDEEP1IN	F	_		_	-	۵	_	_	*
volume)		M		_	_	^	_	_	_	*
Mass transfer out of 1st deep lung compartment (L/hr; scaled to tissue	KLNGDEEP1OUT	F	-	_	-	^	_	-	_	*
volume)		M	-	_	_	(_	_	_	^
Mass transfer parameter into 1st deep lung compartment (L/hr;	KLIVDEEP1IN	F			-	h	•		_	-
scaled to tissue volume)	KLIVDEEI IIIV	M			_	*			_	_
Mass transfer parameter into 2nd	W W DEEpany	F	-		_	(_		-	_
deep liver compartment (L/hr; scaled to tissue volume)	KLIVDEEP2IN	M	-		_	(_		-	_
Mass transfer parameter out of 1st	W WEEDLOVE	F	-	(P)	_	_	۵	O P	-	_
deep liver compartment (L/hr; scaled to tissue volume)	KLIVDEEP1OUT -	M	-		_	_	۵	O P	-	_
Mass transfer parameter out of 2nd	W W D D D D D D D D D D D D D D D D D D	F	-		_	^	_		-	_
deep liver compartment (L/hr; scaled to tissue volume)	KLIVDEEP2OUT	M	-	e'	-	h	_		_	_
Maximal capacity (mg/hr/BW0.75)	VMAXC	F			95	^	_		33	*
Waximar capacity (mg/m/b w 0.75)	VIVITATE	M			33	*			98	*
Maximum CYP production rate	KMAX	F			33	*	_	_	93	*
(AUC/hr/μg protein)	KWAX	M			35	_	۵		93	*
Metabolite volume of distribution	VDISTC	F	-	_	_	(1)	_	_	_	_
(L/kg)	VDISTC	M	-	_	_	*	_	_	_	_
Production of MLP in liver (distributed and diffuse) (L/hr;	KMLP	F	ı	_	_	(_	_	_
scaled to tissue volume)	KMLP	M	I	-	-	^		_	-	_
Production of MLP in fat	WMI DE	F		_	_	^	•	_	_	_
(distributed and diffuse) (L/hr; scaled to tissue volume)	KMLPF	M		_	-	(•	_	_	_
Production rate of MLP in deep	KMLPDEEP	F		-	-	^	•	-	-	_
liver (L/hr; scaled to tissue volume)		M		_	_	*		_	_	_
Rapidly perfused volume (fraction	VRAPC	F	-	O	35	-	•	_	33	*
of BW)		M	-		35	*			93	M
	PRAPAIR	F	I	_	_	(1)	_	_	_	_

Parameter (uni	ts)	Label	Sex	E	nd of I	Exposu	re	_	2 Week nd of E		•
Rapidly perfused:air part coefficient (unitless)	ition		M	_	_	_	*	_	_	_	_
Slowly perfused tissue di coefficient (fraction of tis		PERMSLW	F		@P	_	(_	_	_	_
flow)		I EKWISE W	M			_	*	_	O P	_	_
Slowly perfused tissue:ai	r partition	PSLWAIR	F			33	_		O P	_	_
coefficient (unitless)		FSLWAIK	M		O P	95	*			_	_
Slowly perfused volume (fraction of		VSLWC	F			8 5	*	•		35	*
BW)		VSLWC	M			95	*	•		3 5	*
Urinary clearance silanol	metabolite	CLURNM1C	F	_	_	_	_	_	_	_	_
1 (L/hr/kg0.75)		CLURIVITE	M	_	_	_	*	_	_	_	_
Urinary clearance silanol	metabolite	CLURNM2C	F	_	_	_	*	_	_	_	_
2 (L/hr/kg0.75)		CLURINIZC	M	_	_	_	*	_	_	_	_
<u>Sensitivity</u>	Compartme	<u>ent</u>									
■ High (>0.5)	♦ Blood										
■ Moderate (0.2–0.5)	Liver										
■ Low (<0.2)	F at										
- 0	h Lungs	↑ Lungs									

Table 4-3. D4 PBPK Model Input Parameters That Result in Normalized Sensitivity Coefficient of 0.2 or Greater in Listed Compartments (Blood, Liver, Fat, and Lung) of SD Rat at the End of 28-day Exposure and the End of 14-day Postexposure Period

904 905

906 907

2 Weeks After Parameter (units) Label Sex **End of Exposure End of Exposure** F 4 1 KM Affinity constant (mg/L) 4 M OP _ OP 4 F 9.0 91 9.0 91 4 QPC Alveolar ventilation (L/hr/kg0.75) M OP 9: 1 949 4 F 91 4 9: 1 Basal CYP degradation rate (hr⁻¹) **KELIMCYP** M 9.0 _ 949 4 F 9.0 01 9.0 01 4 4 Basal CYP production rate **K**0 (AUC/hr/µg protein) M 9.0 4 P 949 4 F 9.0 01 4 9.0 4 Blood flow in diffuse fat (fraction of **QFATDIFFC** BW) M 20 4 4 F 94 4 앩 4 Blood flow in distributed fat (fraction **QFATDISTC** of BW) M 9.9 Si. 4 4 F 0.0 **31** 4 Blood flow in liver (fraction of BW) **QLIVC** M _ 9.9 01 4 Si. _ F 9: Si. 4 **QRAPC**

Parameter (units)	Label	Sex	E	nd of I	Exposu	re		2 Week and of E		
Blood flow in rapidly perfused tissues (fraction of BW)		M	_	@P	33	_		@P	31	*
Blood flow in slowly perfused tissues	OCI WG	F			33	^	۵		35	(
(fraction of BW)	M	35	*			31	h			
Blood volume (fraction of BW)	VBLDC	F		_	_	_	•	_	_	_
Blood volume (naction of B w)	VBLBC	M		_	_	(•	-	_	-
Blood:air partition coefficient	PBLD		•	-	35	*	•		31	(
(unitless)				-	33	_	•		31	(
Body weight (kg)	BW				35	_		OP -	35	(
					35	-		OP -	35	(
Cardiac output (L/hr/kg0.75)	QCC			-	36	/			35	(1)
					95	^			8	(
Clearance from MLP compartment to		F		_	_	_		_	_	_
fat (distributed and diffuse) (L/hr; scaled to tissue volume)	KREMOVALFMLP	M		_	_	()	•	_	_	_
Clearance from MLP compartment to	VIDEO (0.01) I VI O	F		_	_	_	۵	_	_	_
liver (L/hr; scaled to tissue volume)	KREMOVALLMLP	M		_	_	4	۵	_	_	_
Diffuse fat diffusion coefficient	DEDME A TIDLEE	F			_	*			_	h
(fraction of tissue blood flow)	PERMITATDIFF	M			_	*			_	*
Diffuse fat volume (fraction of BW)	VEATDIFFC	F		O P	33	_	•		33	h
Diriuse fat volume (fraction of DW)	VIAIDIIIC	M			33	(1)			33	*
Diffuse fat:air partition coefficient	PEATDIEEA IR	F	-	_	_	*		_	_	h
(unitless)	TAIDHTAIK	M	_	_	_	*		_	_	*
Dissociation constant CYP induction	KDLIV	F			_	_			_	_
(μΜ)	KDEI V	M			_	*			_	_
Distributed fat diffusion coefficients	PERMEATDIST	F	_	_	95	_			31	*
(fraction of tissue blood flow)	TERMI ATDIST	M	_	_	35	(1)	_	O P	3 5	*
Distributed fat volume (fraction of	VEATDISTC	F	_	_	35	*			3 5	h
BW)	VIAIDISIC	M	_	_	35	(1)		O P	3 5	*
Distributed fat:air partition coefficient	PFATDISTAIR	F	•	_	31	^	•		31	^
(unitless)		M	_	_	31	*			31	M
Fecal excretion of metabolite (1 and 2)	KFECSCLSC	F	-	_	_	M	_	_	-	_
(BW-0.25/hr)		М	_	_	_	_	_	_	_	_
Fraction of mass returning from 1st deep liver compartment available for	FRLIDM	F			_	_		_	_	_
metabolism (unitless)		M			_	M		_	-	_
	CYP0	F			35	*			8 6	*

Parameter (units)	Label	Sex		nd of I	Exposu	re		2 Week nd of E		
Induction of metabolism in liver, basal level of CYP (AUC/µg protein)		M	۵		95	h	•		0.0	^
level of CTP (AUC/µg protein)		F	A		3:	()	_	_	_	_
Inhalation concentration (ppm)	CONC	M			35	A	•	@	35	^
		F	•		_	()	•		33	*
Liver volume (fraction of BW)	VLIVC	M		@P	_	_	۵	O P	33	(
Liver:air partition coefficient	DI WAA ID	F			33	H	•		33	(
(unitless)	PLIVAIR	M			35	_	۵		33	(
Lung volume (fraction of BW)	VLNGC	F	-	_	_	*		_	33	-
Lung volume (maction of bw)	VENGC	M	-	_	_	_		_	33	_
Lung:air partition coefficient (unitless)	PLNGAIR	F	_	_	_	*	_	_	_	^
Zung.un partition coefficient (unitiess)	T Zi (Grint	M	_	_	_	*	_	_	_	*
Mass transfer into 1st deep lung compartment (L/hr; scaled to tissue	KLNGDEEP1IN	F	_	_	_	*	_	_	_	*
volume)	KENODELI IIIV	M	_	_	_	*	_	_	_	*
Mass transfer out of 1st deep lung		F	-	_	_	*	_	_	_	*
compartment (L/hr; scaled to tissue volume)	KLNGDEEP1OUT	M	-	-	-	h	-	-	-	*
Mass transfer parameter into 1st deep		F			33	(•		33	(
lung compartment (L/hr; scaled to tissue volume)	KLIVDEEP1N	M			98	_	•		33	*
Mass transfer parameter into 2nd deep	W WDEEDADY	F	-		_	(1)	_		_	_
liver compartment (L/hr; scaled to tissue volume)	KLIVDEEP2IN	M	_		_	*	_		_	-
Mass transfer parameter out of 1st		F	-	O P	_	(1)			_	-
deep liver compartment (L/hr; scaled to tissue volume)	KLIVDEEP1OUT	M	_		_	h	•		-	_
Mass transfer parameter out of 2nd		F	_		_	_	_		_	-
deep liver compartment (L/hr; scaled to tissue volume)	KLIVDEEP2OUT	M	_	(P)	_	A	_		_	_
	VD 4.1 V.G	F			33	(۵		33	(
Maximal capacity (mg/hr/BW0.75)	VMAXC	M			35	*	۵		33	(
Maximum CYP production rate	KMAX	F			33	*		@P	33	*
(AUC/hr/µg protein)	KWAA	M		O P	95	*		O P	33	^
Metabolite volume of distribution	VDISTC	F	_	_	_		_	_	_	_
(L/kg)	-	M	_	_	_	M	_	_	_	_
Production of MLP in liver (distributed and diffuse) (L/hr; scaled	KMLP	F M		_	_	_		_	_	
to tissue volume)		F	<u> </u>	_	_	(h)		_	_	_
Production of MLP in fat (distributed and diffuse) (L/hr; scaled to tissue	KMLPF	M	•	_	_		•	_	_	
volume)		IVI				*		_		

Parameter (units)	Label	Sex	E	nd of I	Exposu	re		2 Week and of E		
Production rate of MLP in deep liver	WM PDEED	F		_	_	*	•	_	_	_
(L/hr; scaled to tissue volume)	KMLPDEEP	M		_	_	_	۵		_	_
Rapidly perfused volume (fraction or	, VID A DC	F	_	_	35	*		-	33	*
BW)	VRAPC	M	_	_	33	*		-	35	*
Rapidly perfused:air partition	DD 4 D 4 ID	F	_	_	_	*	_	_	_	_
coefficient (unitless)	PRAPAIR	M	_	_	_	4	_	_	_	_
Slowly perfused tissue diffusion coefficient	PERMSLW	F			_	_			_	_
(fraction of tissue blood flow)	F ERWISE W	M		O P	_	(_	_
Slowly perfused tissue:air partition	DGI WAAD	F			33	*			_	_
coefficient (unitless)	PSLWAIR	M		O P	33	*			_	_
Slowly perfused volume (fraction of	NOT WAS	F			33	_	۵		31	*
BW)	VSLWC	M		O P	33	*	۵		31	*
Urinary clearance silanol metabolite	1 (7.17)	F	_	_	_	(_	_	_	_
(L/hr/kg0.75)	CLURNM1C	M	_	_	_	(_	_	_	_
Urinary clearance silanol metabolite	2 CLURNM2C	F	_	_	-	*	_	_	_	-
(L/hr/kg0.75)	CLURNM2C	M	_	_	_	_	_	_	_	_
Sensitivity Compartm	<u>ent</u>									
■ High (>0.5)										
■ Moderate (0.2–0.5)										_
Low (<0.2)										
− 0 Lungs										

Table 4-4. D4 PBPK Model Input Parameters That Result in a Normalized Sensitivity Coefficient of 0.2 or Greater Listed Compartments (Exhaled Breath, Plasma) of Human Male at the End of Dermal Exposure and the End of Postexposure Period

908 909

910

911

7 Hours after Parameter (units) Label **End of Exposure End of Exposure** KSKNBLD Absorption into blood from skin (cm/hr) **(** lacktriangleAffinity constant (mg/L) KMAGE Age **P** 4 **₽** Alveolar ventilation (L/hr/kg0.75) QPC Basal CYP production rate (AUC/hr/µg protein) K0 QFATDIFFC Blood flow in diffuse fat (fraction of BW) 4

Parameter (units)	Label	End of E	Exposure		Hours after of Exposure		
Blood flow in liver (fraction of BW)	QLIVC		6		P		
Blood flow in rapidly perfused tissues (fraction of BW)	QRAPC	\$	6	*	P		
Blood flow in slowly perfused tissues (fraction of BW)	QSLWC		P	4	P		
Blood volume (fraction of BW)	VBLDC		6	_	6		
Blood:air partition coefficient (unitless)	PBLD		6	\$	6		
Body weight (kg)	BW		6	\$	6		
Clearance from MLP compartment to fat (distributed and diffuse) (L/hr; scaled to tissue volume)	KREMOVALFMLP	_	_	_	P		
Clearance from MLP compartment to liver (L/hr; scaled to tissue volume)	KREMOVALLMLP	_	_	*	6		
Dermal exposure surface area 1st location (cm ²)	DERMAREA1	*	6	*	6		
Dermal exposure surface area 2nd location (cm ²)	DERMAREA2	-	_	*	6		
Diffuse fat diffusion coefficient (fraction of tissue blood flow)	PERMFATDIFF	_	_	(4)	P		
Diffuse fat volume (fraction of BW)	VFATDIFFC	\$	6	*	6		
Diffuse fat:air partition coefficient (unitless)	PFATDIFFAIR	_	_	*	P		
Evaporation rate from skin surface (cm/hr)	KEVAPC	-	_	*	P		
Fraction of mass returning from 1st deep liver compartment available for metabolism (unitless)	FRLIDM	_	_	_	P		
Induction of metabolism in liver, basal level of CYP (AUC/ μ g protein)	CYP0	_	_	_	6		
Liver volume (fraction of BW)	VLIVC	_	_	*	P		
Liver:air partition coefficient (unitless)	PLIVAIR	-	6	_	P		
Lung volume (fraction of BW)	VLNGC		(*	P		
Lung:air partition coefficient (unitless)	PLNGAIR	\$	6	\$	_		
Mass transfer into 1st deep lung compartment (L/hr; scaled to tissue volume)	KLNGDEEP1IN	_	_	*	_		
Mass transfer out of 1st deep lung compartment (L/hr; scaled to tissue volume)	KLNGDEEP1OUT	_	_	(4)	_		

Parameter	(units)	Label	End of E	Exposure		rs after Exposure
Mass transfer parameter into compartment (L/hr; scaled to		KLIVDEEP1IN	_	_	_	6
Mass transfer parameter out of compartment (L/hr; scaled to		KLIVDEEP1OUT	_	_	_	6
Maximal capacity (mg/hr/BW	70.75)	VMAXC	_	_		P
Out of deep skin compartmen	t (hr ⁻¹)	KSKNINC	*	6	\$	6
Production of MLP in fat (dis (L/hr; scaled to tissue volume		KMLPF	_	_	*	6
Production rate of MLP in de (L/hr; scaled to tissue volume		KMLPDEEP	_	_	-	6
Production of MLP in liver (L/hr; scaled to tissue volume	·)	KMLP	_	_	_	6
Rapidly perfused volume (fra	ction of BW)	VRAPC	*	6	*	6
Rapidly perfused:air partition	coefficient (unitless)	PRAPAIR	*	P	_	6
Rate constant of transfer into (/hr)	deep skin compartment	KSKNDEEPIN	*	P	*	P
Rate constant of transfer out of compartment (/hr)	of deep skin	KSKNDEEP OUT	_	_	\$	_
Rate evaporated from skin tis	sue (cm/hr)	KSKNOUTC	_	_	\$	6
Slowly perfused tissue diffus (fraction of tissue blood flow		PERMSLW	*	P	*	P
Slowly perfused tissue:air par (unitless)	rtition coefficient	PSLWAIR	_	_	*	P
Slowly perfused volume (frac	ction of BW)	VSLWC	*	P	\$	6
<u>Sensitivity</u>	Compartment					<u>I</u>
■ High (>0.5)	Breath					
■ Moderate (0.2–0.5)	6 Plasma					
Low (<0.2)						
- 0						

Table 4-5. D4 PBPK Model Input Parameters That Result in a Normalized Sensitivity Coefficient of 0.2 or Greater in Listed Compartments (Exhaled Breath, Plasma) of Human Male at the End of Inhalation Exposure and the End of Postexposure Period

912

913

914

Parameter (units)	Label	End of Exposure		7 Hour End of E	
A binary to use human exercise equations (unitless)	HUMANEX	\$	6	*	6

Parameter (units)	Label	End of E	Exposure	7 Hours after End of Exposure		
Affinity constant (mg/L)	KM	\$	P	\$	P	
Age (years)	AGE	\$	6	\$	6	
Basal CYP degradation rate (hr ⁻¹)	KELIMCYP	*	_	*	_	
Basal CYP production rate (AUC/hr/µg protein)	КО		_	*	_	
Blood flow in diffuse fat (fraction of BW)	QFATDIFFC		_	\$	_	
Blood flow in liver (fraction of BW)	QLIVC		6	\$	6	
Blood flow in rapidly perfused tissues (fraction of BW)	QRAPC		6	*	(
Blood flow in slowly perfused tissues (fraction of BW)	QSLWC	-	P	*	P	
Blood volume (fraction of BW)	VBLDC	*	6	-	6	
Blood:air partition coefficient (unitless)	PBLD	*	6	*	6	
Body weight (kg)	BW	*	6	*	(
Clearance from MLP compartment to fat (distributed and diffuse) (L/hr; scaled to tissue volume)	KREMOVALFMLP	\$	_	-	P	
Clearance from MLP compartment to liver (L/hr; scaled to tissue volume)	KREMOVALLMLP		_	*	6	
Diffuse fat diffusion coefficient (fraction of tissue blood flow)	PERMFATDIFF	*	6		6	
Diffuse fat volume (fraction of BW)	VFATDIFFC		P		6	
Diffuse fat:air partition coefficient (unitless)	PFATDIFFAIR		_		P	
Dissociation constant CYP induction (µM)	KDLIV		-	*	_	
Fecal excretion of metabolite (1 and 2) (BW-0.25/hr)	KFECSCLSC	*	_	_	_	
Fraction of mass returning from 1st deep liver compartment available for metabolism (unitless)	FRLIDM		-	\$	P	
Induction of metabolism in liver, basal level of CYP (AUC/µg protein)	CYP0		6		P	
Inhalation concentration (ppm)	CONC	*	6	*	6	
Liver volume (fraction of BW)	VLIVC	\$	_	\$	(P)	
Liver:air partition coefficient (unitless)	PLIVAIR		-		P	

Parameter (un	iits)	Label	End of E	Exposure	7 Hour End of E	
Lung volume (fraction of BW)		VLNGC	\$	6	\$	P
Lung:air partition coefficient (un	itless)	PLNGAIR	*	6	*	_
Mass transfer into 1st deep lung (L/hr; scaled to tissue volume)	compartment	KLNGDEEP1IN		_	_	-
Mass transfer out of 1st deep lun (L/hr; scaled to tissue volume)	g compartment	KLNGDEEP1OUT	\$	_	*	_
Mass transfer parameter into 1st compartment (L/hr; scaled to tiss		KLIVDEEP1IN	*	_	*	P
Mass transfer parameter into 2nd compartment (L/hr; scaled to tiss		KLIVDEEP2IN	*	_	_	_
Mass transfer parameter out of 1 compartment (L/hr; scaled to tiss		KLIVDEEP10UT	*	_	*	P
Maximal capacity (mg/hr/BW0.7	75)	VMAXC	\$	6		P
Maximal capacity (mg/hr/BW0.7	75)	KMAX		_	_	_
Metabolite volume of distributio	n (L/kg)	VDISTC	\$	_	_	_
Production of MLP in fat (distrib (L/hr; scaled to tissue volume)	outed and diffuse)	KMLPF		6	\$	6
Production rate of MLP in deep (L/hr; scaled to tissue volume)	liver	KMLPDEEP	\$	_	_	P
Production of MLP in liver (L/hr; scaled to tissue volume)		KMLP	_	_	_	P
Rapidly perfused volume (fraction	on of BW)	VRAPC		6	\$	P
Rapidly perfused:air partition co	efficient (unitless)	PRAPAIR		P	*	P
Slowly perfused tissue diffusion (fraction of tissue blood flow)	coefficient	PERMSLW	*	(*	_
Slowly perfused tissue:air partiti (unitless)	on coefficient	PSLWAIR	-	_	*	-
Slowly perfused volume (fraction	n of BW)	VSLWC	\$	6		Ø
Urinary clearance silanol metabo	olite 1 (L/hr/kg0.75)	CLURNM1C	*	_	_	_
Urinary clearance silanol metabo	olite 2 (L/hr/kg0.75)	CLURNM2C		_	_	_
Sensitivity	Compartment	l	1	1		
■ High (>0.5)	* Breath					
■ Moderate (0.2–0.5)	O Plasma					
Low (<0.2)	• I lasilla					

917 Table 4-6. D4 PBPK Model Input Parameters That Result in a Normalized Sensitivity Coefficient 918

of 0.2 or Greater in Listed Compartments (Exhaled Breath, Plasma) of Human Male at the End of

Oral Exposure and the End of Postexposure Period

Parameter (units) Affinity constant (mg/L)	Label KM	End of Exposure		7 Hours after End of Exposure	
		\$	6	\$	P
Alveolar ventilation (L/hr/kg0.75)	QPC	*	6	\$	P
Basal CYP degradation rate (/hr)	KELIMCYP		_		P
Basal CYP production rate (AUC/hr/µg protein)	K0		_		P
Blood flow in diffuse fat (fraction of BW)	QFATDIFFC		_	*	_
Blood flow in liver (fraction of BW)	QLIVC	*	6	*	P
Blood flow in rapidly perfused tissues (fraction of BW)	QRAPC	*	6	*	P
Blood flow in slowly perfused tissues (fraction of BW)	QSLWC		6	\$	P
Blood volume (fraction of BW)	VBLDC		6	\$	P
Blood:air partition coefficient (unitless)	PBLD		6	*	P
Body weight (kg)	BW	\$	6	*	P
Cardiac output (L/hr/kg0.75)	QCC	\$	6	*	P
Clearance from MLP compartment to fat (distributed and diffuse) (L/hr; scaled to tissue volume)	KREMOVALFMLP	-	_	_	P
Clearance from MLP compartment to liver (L/hr; scaled to tissue volume)	KREMOVALLMLP	_	_	_	P
Diffuse fat diffusion coefficient (fraction of tissue blood flow)	PERMFATDIFF	\$	-	-	P
Dissociation constant CYP induction (μM)	KDLIV		_	\$	P
Fraction of mass returning from 1st deep liver compartment available for metabolism (unitless)	FRLIDM	-	_		P
Induction of metabolism in liver, basal level of CYP (AUC/µg protein)	CYP0		6	*	P
Length administration oral dose (hr)	ORALPULSETIME	*	6	\$	P
Liver volume (fraction of BW)	VLIVC		6	\$	P
Liver:air partition coefficient (unitless)	PLIVAIR	*	P	\$	P

Parameter (units)	Label	End of Exposure		7 Hours after End of Exposure	
Lung volume (fraction of BW)	VLNGC	\$	-	_	_
Lung:air partition coefficient (unitless)	PLNGAIR	*	_	_	P
Mass transfer into 1st deep lung compartment (L/hr; scaled to tissue volume)	KLNGDEEP1IN	_	_	*	P
Mass transfer parameter into 1st deep lung compartment (L/hr; scaled to tissue volume)	KLIVDEEP1IN	*	_	*	P
Mass transfer parameter out of 1st deep liver compartment (L/hr; scaled to tissue volume)	KLIVDEEP1OUT	*	ı	*	P
Maximal capacity (mg/hr/BW0.75)	VMAXC	*	P	*	P
Maximal capacity (mg/hr/BW0.75)	KMAX		-	\$	P
Oral absorption rate 1st compartment (/hr)	KABS	*	P	*	P
Oral absorption rate 1st lipoprotein-associated compartment (/hr)	KABSL	*	6		P
Oral absorption rate 2nd compartment (/hr)	K2ABS	*	P	*	P
Oral absorption rate transfer 1st to 2nd compartment (/hr)	KABS2	*	P	*	6
Oral absorption rate transfer from free to lipoprotein-associated absorption (/hr)	KORTOL	\$	O	\$	P
Oral dose (mg/kg)	PDOSEC	\$	P	\$	P
Production of MLP in fat (distributed and diffuse) (L/hr; scaled to tissue volume)	KMLPF	_	-	_	6
Production rate of MLP in deep liver (L/hr; scaled to tissue volume)	KMLPDEEP	_	_	_	P
Production of MLP in liver (L/hr; scaled to tissue volume)	KMLP	_	_	_	P
Rapidly perfused tissue:air partition coefficient (unitless)	PRAPAIR		_	\$	_
Rapidly perfused volume (fraction of BW)	VRAPC	\$	_	\$	P
Rate constant for absorption rate 2nd lipoprotein-associated compartment (/hr)	K2ABSL	_	P	*	P
Rate constant for fecal excretion of unabsorbed oral dose (/hr)	KFEC	_	-	\$	P
Rate constant for transfer 1st to 2nd lipoprotein- associated compartment (/hr)	KABS2L	*	P	*	P
Slowly perfused tissue diffusion coefficient (fraction of tissue blood flow)	PERMSLW		_	*	_
Slowly perfused volume (fraction of BW)	VSLWC	*	P	\$	P

Parameter (units	()	Label	abel End of Exposu		7 Hours after End of Exposure		
Uptake into deep blood compartment from oral absorption lipid (L/hr; scaled to tissue volume)		KREMOVALF	*	P	*	P	
Uptake into distributed fat compartment from oral absorption lipid (L/hr; scaled to tissue volume)		KREMOVALF DIST	*	P	*	P	
Uptake into fraction of liver compartment removal to 1st deep liver compartment (L/hr; scaled to tissue volume)		FRACOLDEEP1	*	P	*	•	
Uptake into liver compartment from oral absorption lipid (L/hr; scaled to tissue volume)		KREMOVALL	*	ø	*	6	
Urinary clearance silanol metabolite 1 (L/hr/kg0.75)		CLURNM1C	_	_	*	P	
Volume of diffuse fat (fraction of BW)		VFATDIFFC		_	*	P	
Sensitivity	Compartment						
■ High (>0.5)	◆ Breath						
■ Moderate (0.2–0.5)	O Plasma						
Low (<0.2)							
- 0							

F344 rats were more sensitive to blood flow parameters both at the end of exposure and in the postexposure period compared with the other parameters—those affecting liver, rapidly perfused, and slowly perfused tissues (QLIVC, QRAPC, and QSLWC, respectively). One possibility is that the lower D4 levels in F344 livers impact the sensitivity of these blood flow parameters. In addition, basal CYP production rate (K0) and maximal CYP production rate (KMAX) result in sensitivity coefficients greater than 0.2 in F344 rats and less than 0.2 in SD rats both at the end of exposure and in the postexposure period. The difference in sensitivity of this parameter between the strains could be explained by experiments that found that D4 is metabolized at lower rates in SD rats compared with F344 rats (Meeks et al., 2022). Specifically, Meeks et al. (2022) observed that CYP2B1/2 and CYP3A1/2 induction and activity are higher in F344 rats relative to SD rats. This observation is reflected in the Campbell model as reduced CYP production rate (KMAX) and the maximum rate of metabolism (VMAXC) in SD rats compared with F344 rats.

The following Venn diagram shows the number of parameters with sensitivity coefficients greater than 0.2 in Table 4-2 through Table 4-6 that are specific to each route and the ones that are common between the routes in humans.

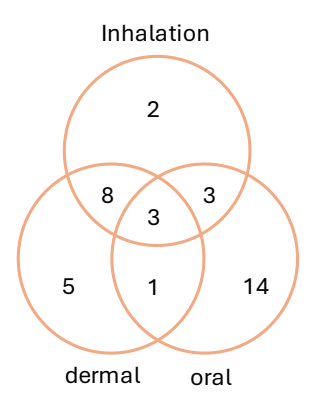


Figure 4-7. Venn Diagram Illustrating the Distribution of Sensitive Parameters by Exposure Route

The oral route shows a different pattern of sensitivity compared with dermal and inhalation routes. Four parameters with sensitivity coefficients greater than 0.2 are oral dose specific in the model, including absorption rate of the 1st compartment [KABS for stomach], transfer from 1st to 2nd compartment [KABS2, transfer rate from stomach to duodenum], transfer from free to lipoprotein-associated absorption [KORTOL], and absorption rate in 1st lipoprotein-associated compartment [KABSL]. Additionally, there are 10 parameters that have SA coefficients greater than or equal to 0.2 only in oral dose, and 8 of these 10 parameters are liver specific. The sensitivity of parameters unique to the oral route may be related to the observation that D4 entry to blood varies by route of exposure (Sarangapani et al., 2003). Orally taken D4 is assumed to be absorbed by chylomicrons or other lipoproteins that may be removed from the blood in the liver, leaving a lower proportion of the absorbed dose available for systemic distribution compared with that from other exposure routes. This sensitivity of parameters specific to the oral route is reflected in the Campbell model with the introduction of the oral absorption submodel to better capture the uptake, distribution, and elimination of D4 in exhaled breath and blood (Campbell et al., 2023; Campbell et al., 2017).

In all three routes of exposure, the exhaled breath is the more sensitive compartment than plasma, and it makes up approximately 77 percent of incidents of the absolute value of the SA coefficient being equal to or exceeding 0.2. The physiological basis of the sensitivity of the exhaled breath compartment is not clear.

 In rats, blood and fat are more sensitive to change in input parameters in the postexposure time period when compared with the end of exposure. In humans, concentrations in plasma and exhaled breath are more sensitive to input parameters in the postexposure period compared with the exposure time period. With respect to species differences, the sensitivity of exhaled breath in humans could potentially relate to differential metabolism; the greater alveolar surface area (57.22 m²) in humans compared with rats (0.297 m²) (U.S. EPA, 2004); differences in the amount of air entering the lungs per minute (minute ventilation), which is lower after adjustment for body weight in humans (0.09–0.13 L/min/kg) compared with rats (0.64–0.8 L/min/kg) (Froehlich et al., 2016); or other physiological differences. One possible explanation of the differential sensitivities between the end of exposure and postexposure periods is that the concentration in body compartments is significantly lower in the postexposure period [Figures 3-7 in (Campbell et al., 2023)]. With low absolute concentration of D4 in the body, any small change in the concentration will result in relatively large SA coefficients.

It is worth noting that compared with the model in McMullin et al. (2016), wherein PFATDIFFAIR = 100 and PFATDISTAIR = 600, the current model values are PFATDIFFAIR = 600

and PFATDISTAIR = 100. Using the values from McMullin et al. (2016) makes small but statistically significant differences in the sensitivity analysis and time-series results.

4.3 Model Applicability

 The Campbell et al. (2023) model predicts experimental data for inhalation, oral, and dermal routes of exposure. It also captures differences in metabolism of D4 between F344 and SD rat strains (Campbell et al., 2023), which is achieved by changing KMAX and VMAXC between the strains (Table 3-3).

Campbell et al. (2023) have predicted the human exposure data for inhalation and dermal routes for which experimental data were available. However, the model can be modified to cover oral exposure, as well, as seen in Figure 4-6.

The model can be used for risk assessment of human exposure to D4 through common routes of exposure, *i.e.*, oral, inhalation, or dermal. However, the model performance for the oral route cannot be assessed. Currently, there are no time-series data for human exposure through oral administration. As discussed in Section 5.1., Dow Corning (1998a) only provided weekly averages for two weeks of exposure with relatively high standard deviation (**Error! Reference source not found.**), rendering the data less useful for model evaluation. The model is developed for healthy adult humans. Further modifications will be needed to address exposure in infants or patients. There are also no specific parameters for pregnancy.

Even in empirical studies, there are uncertainties in human dermal exposure outcomes. The current model uses data from Plotzke et al. (2000) (as cited in Reddy et al. (2007)), wherein relatively significant amounts of D4 were measured in exhaled breath of human subjects after a dermal exposure. In contrast, in a similar study by Biesterbos et al. (2015), no significant amount of D4 was observed in the exhaled breath. The difference in the results may be due to different exposure scenarios. Plotzke et al. (2000) (as cited in Reddy et al. (2007)) applied 1 to 1.4 g of D4 to the two axillae whereas in Biesterbos et al. (2015), 2.5 mg of D4 per cm² were applied to the forearm for 1 hour to achieve an accumulated exposure of 15 mg/cm². Therefore, the dermal model should be used with caution.

5 DISCUSSION AND CONCLUSIONS

In previous versions of the model, the MLP compartment was a unidirectional compartment that allowed transfer of D4 in blood from the liver to fat. In addition, the D4 cleared from the fat was assumed to be unbound in the blood and eventually exhaled. As a result, the model underestimated the amount of D4 in plasma and fat in the 14-day post-exposure period. Campbell and colleagues speculated that "the unidirectional [sic] description did not capture the reverse process, in which lipids in adipose and other tissues are transported to the liver as high-density lipoproteins and D4 associated with it." Therefore, bidirectional exchange between MLP and liver and MLP and fat compartments was incorporated, and the related parameters such as KMLP, KMLPF, KMLPDEEP, KREMOVALLMLP and KREMOVALFMLP, and PERMFATDIFF were optimized to achieve more accurate prediction of the experimental data, particularly in plasma and fat (Campbell et al., 2023).

An important parameter in human exposure studies is the age of subjects. In the current model, age directly influences only the cardiac output to the tissues during rest or exercise states. However, one would expect parameters such as tissue volume, tissue uptake, metabolism rate, or partition coefficients to change with age. Additional modifications need to be made to account for those factors.

EPA successfully reproduced published data using this model, indicating the model as implemented is sufficient for analysis of D4 toxicokinetics for risk assessment purposes. The model can be used for risk assessment of human exposure to D4 through common routes of exposure. Its predictions are mostly accurate for healthy adult humans in normal conditions, but it has not been tested on pregnant women, infants, or the elderly.

6 LIST OF ELECTRONIC FILES AND SUPPORTING DOCUMENTS 1027

R scripts that were used for local sensitivity analysis and calculation of the model residuals are included in "Model evaluation codes.zip," attached to this report. 1028 1029

REFERENCES

- Andersen, ME. (2022). Assessing modes of action, measures of tissue dose and human relevance of rodent toxicity endpoints with octamethylcyclotetrasiloxane (D4) [Review]. Toxicol Lett 357: 57-72. http://dx.doi.org/10.1016/j.toxlet.2021.12.020
- 1034 Andersen, ME; Sarangapani, R; Reitz, RH; Gallavan, RH; Dobrev, ID; Plotzke, KP. (2001).
 1035 Physiological modeling reveals novel pharmacokinetic behavior for inhaled
 1036 octamethylcyclotetrasiloxane in rats. Toxicol Sci 60: 214-231.

1037 http://dx.doi.org/10.1093/toxsci/60.2.214

- Biesterbos, JW; Beckmann, G; van Wel, L; Anzion, RB; von Goetz, N; Dudzina, T; Roeleveld, N; Ragas, AM; Russel, FG; Scheepers, PT. (2015). Aggregate dermal exposure to cyclic siloxanes in personal care products: Implications for risk assessment. Environ Int 74: 231-239. http://dx.doi.org/10.1016/j.envint.2014.10.017
- <u>Bio-Research Laboratories LTD.</u> (1996a). Method development for the determination of 14C-octamethylcyclotetrasiloxane (D4) pharmacokinetics in the rat following single nose-only vapor inhalation exposure to 14C-D4. (1995-I0000-41000). Midland, MI: Dow Corning Corporation.
- <u>Bio-Research Laboratories LTD.</u> (1996b). Pharmacokinetics of 14C-octamethylcyclotetrasiloxane (D4) in the rat followinng single nose-only vapor inhalation exposure to 14C-D4 at 3 dose levels, w/cvr ltr dated 10/14/96 [TSCA Submission]. (1995-I0000-40999. OTS0558922. 86970000024. TSCATS/444970). Dow Corning Corporation.
- <u>Bois, FY.</u> (2009). GNU MCSim: Bayesian statistical inference for SBML-coded systems biology models. Bioinformatics 25: 1453-1454. http://dx.doi.org/10.1093/bioinformatics/btp162
- Brooke, DN; Crookes, MJ; Gray, D; Robertson, S. (2009). Environmental risk assessment report:

 Octamethylcyclotetrasiloxane. Bristol, UK: UK Environmental Agency.

 https://assets.publishing.service.gov.uk/government/uploads/system/uploads/attachment_data/file/290565/scho0309bpqz-e-e.pdf
- Brown, RP; Delp, MD; Lindstedt, SL; Rhomberg, LR; Beliles, RP. (1997). Physiological parameter values for physiologically based pharmacokinetic models [Review]. Toxicol Ind Health 13: 407-484. http://dx.doi.org/10.1177/074823379701300401
- Butts, M; Cella, J; Wood, CD; Gillette, G; Kerboua, R; Leman, J; Lewis, L; Rajaraman, S; Rubinsztajn, S; Schnattenmann, F; Stein, J; Wengrovius, J; Wicht, D. (2003). Silicones. In HF Mark (Ed.), Encyclopedia of polymer science and technology (4th ed., pp. 765-841). Hoboken, NJ: John Wiley & Sons Inc. http://dx.doi.org/10.1002/0471440264.pst338
- Campbell, J; Andersen, M; Gentry, R; Landingham, CV; Clewell, H. (2023). Incorporation of a recirculating mobile lipid pool description into the cyclic volatile siloxane (cVMS) PBPK model captures terminal clearance of D4 after repeated inhalation exposure in F344 and SD Rats. Toxicol Lett 375: 29-38. http://dx.doi.org/10.1016/j.toxlet.2022.12.014
- Campbell, JL; Andersen, ME; Van Landingham, C; Gentry, R; Jensen, E; Domoradzki, JY; Clewell, HJ. (2017). Refinement of the oral exposure description in the cyclic siloxane PBPK model for rats and humans: Implications for exposure assessment. Toxicol Lett 279 Suppl. 1: 125-135. http://dx.doi.org/10.1016/j.toxlet.2017.04.002
 - CES. (2005). Octamethylcyclotetrasiloxane (D4) (Submission No. 1). Brussels: Centre Européen des Silicones and the European Cosmetic Toiletry and Perfumery Association (COLIPA).
- 1072 <u>CIIT.</u> (2005). Non-regulated study: Assessment of cyclic siloxane activation of the constitutive 1073 androstane receptor. (9963-102). Reston, VA: Silicones Environmental, Health and Safety 1074 Council.
- ClinTrials. (1997). Pharmacokinetics of 14C-octamethylcyclotetrasiloxane (D4) in the rat following 14 repeat daily nose-only vapor inhalation exposures to unlabeled D4 and a single exposure (day 15) to 14C-D4 at two dose levels. (1996-I0000-42577; 8451). Midland, MI: Dow Corning Corporation.

- Dobrev, ID; Nong, A; Liao, KH; Reddy, MB; Plotzke, KP; Andersen, ME. (2008). Assessing kinetic determinants for metabolism and oral uptake of octamethylcyclotetrasiloxane (D4) from inhalation chamber studies. Inhal Toxicol 20: 361-373.

 http://dx.doi.org/10.1080/08958370801903743
- 1083 <u>Domoradzki, JY; Sushynski, A; Sushynski, AA; McNett, DA; Van Landingham, C; Plotzke, KP.</u> (2017). 1084 Metabolism and disposition of [14C]-methylcyclosiloxanes in rats. Toxicol Lett 279(Suppl. 1): 1085 98-114. http://dx.doi.org/10.1016/j.toxlet.2017.05.002
- 1086 Dow Corning. (1990). A 14-day subchronic oral gavage study with octamethylcyclotetrasiloxane in rats [TSCA Submission]. (OTS0528331. 86-910000037. TSCATS/413314). https://ntrl.ntis.gov/NTRL/dashboard/searchResults/titleDetail/OTS0528331.xhtml
- Dow Corning. (1994). 4-Hour acute inhalation toxicity study with octamethylcyclotetrasiloxane in rats with cover letter dated 11/21/94 [TSCA Submission]. (1994-I0000-39679. OTS0557551. 86950000038. TSCATS/443022). Dow Corning Corp.
- 1092 <u>Dow Corning.</u> (1998a). Non-regulated study: Immune effects of oral exposure of human volunteers to octamethylcyclotetrasiloxane (D4), with cover letter dated 12/04/1998 [TSCA Submission]. (1998-I0000-45117. OTS0573865. 86990000015. TSCATS/453872).
- 1095 Dow Corning. (1998b). An oral gavage study to compare the absorption potential of 14c-1096 octamethylcyclotetrasiloxane in Fischer 344 rats when delivered in various carriers, with cover 1097 letter dated 9/18/1998 [TSCA Submission]. (OTS0559519. 86980000184. TSCATS/445660).
- Dow Corning. (2001a). Effects of repeated whole body inhalation exposure to
 octamethylcyclotetrasiloxane vapors on hepatic microsomal CYP2b1/2 induction in female rats:
 a dose-response study, w/cover letter dated 021401 [TSCA Submission]. (Report Number 2000-10000-48438. Study Number 8850. OTS0574198. 86010000002. TSCATS/454384). Dow
 Corning Corp.
 Dow Corning. (2001b). In vivo percutaneous absorption of 14C-octamethylcyclotetrasiloxane in the rat,

1104 1105

1106 1107

1108

- <u>Dow Corning.</u> (2001b). In vivo percutaneous absorption of 14C-octamethylcyclotetrasiloxane in the rat, with cover letter dated 021901 [TSCA Submission]. (OTS0574205. 86010000009. TSCATS/454392).
- <u>Dow Corning.</u> (2001c). Support: A five-week inhalation study in multiple species with octamethylcyclotetrasiloxane (D4), with cover letter dated 043001 [TSCA Submission]. (Report No. 1999-I0000-47921. Study No. 7484. OTS0557019-1. 87010000002. TSCATS/454382). Dow Corning Corp.
- Dow Corning. (2002). Initial submission: Effects of octamethylcyclosiloxane on cell proliferation in the liver of female Fischer 344 rats: a 28-day inhalation study, with cvr ltr dtd 120202 [TSCA Submission]. (2002-I0000-52111. 8491. OTS0001439. FYI-1202-01439. TSCATS/454960). Dow Corning Corp.
- Dow Corning. (2004). Letter Re: Supplemental submission of final report to 8EHQ-02-15088 TSCA
 Section 8e notification of substantial risk: Octamethylcyclotetrasiloxane [TSCA Submission].
 (89-050000046. 8EHQ-1104-15088).
- 1117 <u>Dow Corning.</u> (2005). Non-regulated study: Assessment of cyclic siloxanes in an In Vitro Pregnane X
 1118 Receptor (PXR) Reporter Gene Assay. (9914-102). Reston, VA: Silicones Environmental,
 1119 Health and Safety Council.
- EC/HC. (2008). Screening assessment for the challenge: Octamethylcyclotetrasiloxane (D4): CASRN 556-67-2. Gatineau, QC: Environment Canada. https://www.ec.gc.ca/ese-ees/2481B508-1760-4878-9B8A-270EEE8B7DA4/batch2_556-67-2_en.pdf
- ECHA. (2016). Opinion on an annex XV dossier proposing restrictions on octamethylcyclotetrasiloxane, decamethylcyclopentasiloxane. (ECHA/RAC/RES-O-0000001412-86-97/D). Helsinki, Finland. https://echa.europa.eu/documents/10162/83df6e5b-e7ae-8279-ed47-e6d92912721c
- Flaningam, OL. (1986). Vapor pressures of poly(dimethylsiloxane) oligomers. Journal of Chemical and Engineering Data 31: 266-272. http://dx.doi.org/10.1021/je00045a002

1128 Franzen, A; Greene, T; Van Landingham, C; Gentry, R. (2017). Toxicology of octamethylcyclotetrasiloxane (D4) [Review]. Toxicol Lett 279 Suppl 1: 2-22.

http://dx.doi.org/10.1016/j.toxlet.2017.06.007

1155

1156

1157

- Froehlich, E; Mercuri, A; Wu, S; Salar-Behzadi, S. (2016). Measurements of Deposition, Lung Surface
 Area and Lung Fluid for Simulation of Inhaled Compounds [Review]. 7: 181.

 http://dx.doi.org/10.3389/fphar.2016.00181
- Gentry, R; Franzen, A; Van Landingham, C; Greene, T; Plotzke, K. (2017). A global human health risk assessment for octamethylcyclotetrasiloxane (D4). Toxicol Lett 279: 23-41. http://dx.doi.org/10.1016/j.toxlet.2017.05.019
- Guo, J; Zhou, Y; Wang, Y; Zhang, B; Zhang, J. (2021). Assessment of internal exposure to methylsiloxanes in children and associated non-dietary exposure risk. Environ Int 154: 106672. http://dx.doi.org/10.1016/j.envint.2021.106672
- Hanssen, L; Warner, NA; Braathen, T; Odland, JØ; Lund, E; Nieboer, E; Sandanger, TM. (2013).

 Plasma concentrations of cyclic volatile methylsiloxanes (cVMS) in pregnant and
 postmenopausal Norwegian women and self-reported use of personal care products (PCPs).
 Environ Int 51: 82-87. http://dx.doi.org/10.1016/j.envint.2012.10.008
- Jean, PA; Plotzke, KP. (2017). Chronic toxicity and oncogenicity of octamethylcyclotetrasiloxane (D4) in the Fischer 344 rat. Toxicol Lett 279 Suppl. 1: 75-97.

 http://dx.doi.org/10.1016/j.toxlet.2017.06.003
- Jovanovic, ML; Mcmahon, JM; Mcnett, DA; Tobin, JM; Plotzke, KP. (2008). In vitro and In vivo percutaneous absorption of super(1) super(4)C-octamethylcyclotetrasiloxane (super(1) super(4)C-D sub(4)) and super(1) super(4)C-decamethylcyclopentasiloxane (super(1) super(4)C-D sub(5)). Regul Toxicol Pharmacol 50: 239-248. http://dx.doi.org/10.1016/j.yrtph.2007.11.003
- Lieberman, MW; Lykissa, ED; Barrios, R; Ou, CN; Kala, G; Kala, SV. (1999). Cyclosiloxanes produce fatal liver and lung damage in mice. Environ Health Perspect 107: 161-165. http://dx.doi.org/10.1289/ehp.99107161
 - McKim, JM; Kolesar, GB; Jean, PA; Meeker, LS; Wilga, PC; Schoonhoven, R; Swenberg, JA; Goodman, JI; Gallavan, RH; Meeks, RG. (2001a). Repeated inhalation exposure to octamethylcyclotetrasiloxane produces hepatomegaly, transient hepatic hyperplasia, and sustained hypertrophy in female Fischer 344 rats in a manner similar to phenobarbital. Toxicol Appl Pharmacol 172: 83-92. http://dx.doi.org/10.1006/taap.2000.9110
- McKim, JM; Wilga, PC; Breslin, WJ; Plotzke, KP; Gallavan, RH; Meeks, RG. (2001b). Potential estrogenic and antiestrogenic activity of the cyclic siloxane octamethylcyclotetrasiloxane (D4) and the linear siloxane hexamethyldisiloxane (HMDS) in immature rats using the uterotrophic assay. Toxicol Sci 63: 37-46. http://dx.doi.org/10.1093/toxsci/63.1.37
- McKim, JM; Wilga, PC; Kolesar, GB; Choudhuri, S; Madan, A; Dochterman, LW; Breen, JG;

 Parkinson, A; Mast, RW; Meeks, RG. (1998). Evaluation of octamethylcyclotetrasiloxane (D4)
 as an inducer of rat hepatic microsomal cytochrome P450, UDP-glucuronosyltransferase, and
 epoxide hydrolase: a 28-day inhalation study. Toxicol Sci 41: 29-41.
 http://dx.doi.org/10.1006/toxs.1997.2398
- McMullin, TS; Yang, Y; Campbell, J; Clewell, HJ; Plotzke, K; Andersen, ME. (2016). Development of an integrated multi-species and multi-dose route PBPK model for volatile methyl siloxanes D4 and D5. Regul Toxicol Pharmacol 74 Suppl: S1-S13.

 http://dx.doi.org/10.1016/j.yrtph.2015.12.010
- Meeks, RG; Jean, PA; Mcnett, DA; Plotzke, KP. (2022). A 28-day whole-body inhalation study to
 evaluate octamethylcyclotetrasiloxane (D4) absorption/distribution in two rat strains. Toxicol
 Lett 370: 53-65. http://dx.doi.org/10.1016/j.toxlet.2022.09.001

- Meeks, RG; Stump, DG; Siddiqui, WH; Holson, JF; Plotzke, KP; Reynolds, VL. (2007). An inhalation reproductive toxicity study of octamethylcyclotetrasiloxane (D4) in female rats using multiple and single day exposure regimens. Reprod Toxicol 23: 192-201. http://dx.doi.org/10.1016/j.reprotox.2006.12.005
- MPI Research. (1999). Estrogenic and antiestrogenic activity of octamethylcyclotetrasiloxane in sprague-dawley and fischer 344 immature female rats using a uterotrophic assay, w/cvr ltr dated 10/14/99 [TSCA Submission]. (MPI Study No. 416-148. 9032. OTS0001362. FYI-OTS-1099-1362. TSCATS/446312). Dow Corning Corporation.
- O'Neil, MJ; Heckelman, PE; Dobbelaar, PH; Roman, KJ; Kenney, CM; Karaffa, LS. (2013). The Merck
 index: An encyclopedia of chemicals, drugs, and biologicals (15th ed.). London, United
 Kingdom: The Royal Society of Chemistry.
- Plotzke, KP; Crofoot, SD; Ferdinandi, ES; Beattie, JG; Reitz, RH; Mcnett, DA; Meeks, RG. (2000).
 Disposition of radioactivity in Fischer 344 rats after single and multiple inhalation exposure to
 [14C]Octamethylcyclotetrasiloxane ([14C]D4). Drug Metab Dispos 28: 192-204.
 - Quinn, AL; Dalu, A; Meeker, LS; Jean, PA; Meeks, RG; Crissman, JW; Gallavan, RH; Plotzke, KP. (2007a). Effects of octamethylcyclotetrasiloxane (D4) on the luteinizing hormone (LH) surge and levels of various reproductive hormones in female Sprague-Dawley rats. Reprod Toxicol 23: 532-540. http://dx.doi.org/10.1016/j.reprotox.2007.02.005
 - Quinn, AL; Regan, JM; Tobin, JM; Marinik, BJ; Mcmahon, JM; Mcnett, DA; Sushynski, CM; Crofoot, SD; Jean, PA; Plotzke, KP. (2007b). In vitro and in vivo evaluation of the estrogenic, androgenic, and progestagenic potential of two cyclic siloxanes. Toxicol Sci 96: 145-153. http://dx.doi.org/10.1093/toxsci/kfl185
- RCC. (1995). 3-Month repeated dose inhalation toxicity study with octamethylcyclotetrasiloxane in rats with a 1-month recovery period [TSCA Submission]. (357637. OTS0557666. 86950000153. TSCATS/443139). Dow Corning Corporation.
 - Reddy, MB; Andersen, ME; Morrow, PE; Dobrev, ID; Varaprath, S; Plotzke, KP; Utell, MJ. (2003). Physiological modeling of inhalation kinetics of octamethylcyclotetrasiloxane in humans during rest and exercise. Toxicol Sci 72: 3-18. http://dx.doi.org/10.1093/toxsci/kfg001
 - Reddy, MB; Dobrev, ID; Mcnett, DA; Tobin, JM; Utell, MJ; Morrow, PE; Domoradzki, JY; Plotzke, KP; Andersen, ME. (2008). Inhalation dosimetry modeling with decamethylcyclopentasiloxane in rats and humans. Toxicol Sci 105: 275-285. http://dx.doi.org/10.1093/toxsci/kfn125
 - Reddy, MB; Looney, RJ; Utell, MJ; Plotzke, KP; Andersen, ME. (2007). Modeling of human dermal absorption of octamethylcyclotetrasiloxane (D-4) and decamethylcyclopentasiloxane (D-5). Toxicol Sci 99: 422-431. http://dx.doi.org/10.1093/toxsci/kfm174
 - <u>Sarangapani, R; Teeguarden, J; Andersen, ME; Reitz, RH; Plotzke, KP.</u> (2003). Route-specific differences in distribution characteristics of octamethylcyclotetrasiloxane in rats: analysis using PBPK models. Toxicol Sci 71: 41-52. http://dx.doi.org/10.1093/toxsci/71.1.41
- Sarangapani, R; Teeguarden, J; Plotzke, KP; Mckim, JM; Andersen, ME. (2002). Dose-response
 modeling of cytochrome P450 induction in rats by octamethylcyclotetrasiloxane. Toxicol Sci 67:
 159-172. http://dx.doi.org/10.1093/toxsci/67.2.159
- SCCS. (2010). Opinion on cyclomethicone Octamethylcyclotetrasiloxane (Cyclotetrasiloxane, D4) and
 Decamethylcyclopentasiloxane (Cyclopentasiloxane, D5). (SCCS/1241/10). Brussels, Belgium:
 European Commission Health & Consumers.
- 1219 https://ec.europa.eu/health/sites/health/files/scientific_committees/consumer_safety/docs/sccs_o_029.pdf
- Schmitt, BG; Tobin, J; Mcnett, DA; Kim, J; Durham, J; Plotzke, KP. (2023). Comparative pharmacokinetic studies of 14C-octamethylcyclotetrasiloxane (14C-D4) in Fischer 344 and Sprague Dawley CD rats after single and repeated inhalation exposure. Toxicol Lett 373: 13-21.
- 1224 http://dx.doi.org/10.1016/j.toxlet.2022.10.008

1190

1191 1192

1193

1194

1195 1196

1197

1201 1202

1203

1204

1205

1206

1207

1208

1209

1210

1211

- 1225 <u>Soetaert, K; Petzoldt, T; Setzer, RW.</u> (2010). Solving differential equations in R: package deSolve. J 1226 Stat Softw 33: 1-25. http://dx.doi.org/10.18637/jss.v033.i09
- 1227 <u>U.S. EPA.</u> (2004). Air quality criteria for particulate matter (Final report, 2004) [EPA Report]. (EPA 600/P-99/002aF-bF). Washington, DC.
 - http://cfpub.epa.gov/ncea/cfm/recordisplay.cfm?deid=87903

1229

1242

- 1230 <u>U.S. EPA.</u> (2022). Final scope of the risk evaluation for octamethylcyclotetrasiloxane
- 1231 (Cyclotetrasiloxane, 2,2,4,4,6,6,8,8-octamethyl-) (D4); CASRN 556-67-2. (EPA 740-R-21-003). Washington, DC: Office of Chemical Safety and Pollution Prevention.
- https://www.epa.gov/system/files/documents/2022-03/casrn_556_67_2-octamethylcyclotetrasiloxane-d4_finalscope.pdf
- University of Rochester Medical Center. (2000). Non-regulated study: Percutaneous absorption studies
 of octamethylcyclotetrasiloxane (D4) using the human skin/nude mouse model, with cover letter
 dt'd 021901 [TSCA Submission]. (1999-I0000-46491. OTS0574199. 86010000003.
 TSCATS/454385). Midland, MI: Dow Corning Corporation.
- 1239 <u>University of Rochester Medical Center.</u> (2001). Non-regulated stdy: Human dermal absorption of octamethylcyclotetrasiloxane (D4), with cover letter dated 021901 [TSCA Submission]. (2000-1241 I0000-49147. OTS0574203. 86010000007. TSCATS/454390). Dow Corning Corporation.
 - <u>University of Rochester Medical Center.</u> (2002). In vitro effects of siloxanes on human immune cells, with cover letter dated 121301. (EPA/OTS Doc #FYI-OTS-0102-01420). Midland, MI: Dow Corning Corporation.
- 1245 <u>Utell, MJ; Gelein, R; Yu, CP; Kenaga, C; Geigel, E; Torres, A; Chalupa, D; Gibb, FR; Speers, DM;</u>
 1246 <u>Mast, RW; Morrow, PE.</u> (1998). Quantitative exposure of humans to an
 1247 octamethylcyclotetrasiloxane (D4) vapor. Toxicol Sci 44: 206-213.
 1248 <u>http://dx.doi.org/10.1006/toxs.1998.2483</u>
- 1249 <u>Varaprath, S; Salyers, KL; Plotzke, KP; Nanavati, S.</u> (1999). Identification of metabolites of octamethylcyclotetrasiloxane (D(4)) in rat urine. Drug Metab Dispos 27: 1267-1273.
- Xu, S; Kropscott, B. (2012). Method for simultaneous determination of partition coefficients for cyclic
 volatile methylsiloxanes and dimethylsilanediol. Anal Chem 84: 1948-1955.
 http://dx.doi.org/10.1021/ac202953t
- Xu, S; Kropscott, B. (2014). Evaluation of the three-phase equilibrium method for measuring
 temperature dependence of internally consistent partition coefficients (KOW, KOA, and KAW)
) for volatile methylsiloxanes and trimethylsilanol. Environ Toxicol Chem 33: 2702-2710.
 http://dx.doi.org/10.1002/etc.2754
- Zhang, Y; Dong, H; Wu, C; Yu, L; Xu, J. (2015). The mixing properties of 1,3,5-trimethyl-1,3,5-tris(3,3,3-trifluoropropyl) cyclotrisiloxane with various organosilicon compounds at different temperatures. J Chem Thermodyn 81: 16-25. http://dx.doi.org/10.1016/j.jct.2014.09.010